



# Upper mantle control on the W isotope record of shallow level plume and intraplate volcanic settings



Mike W. Jansen<sup>a,\*</sup>, Jonas Tusch<sup>a</sup>, Carsten Münker<sup>a</sup>, Alessandro Bragagni<sup>a,b</sup>, Riccardo Avanzinelli<sup>b</sup>, Filippo Mastroianni<sup>b</sup>, Finlay M. Stuart<sup>c</sup>, Florian Kurzweil<sup>a</sup>

<sup>a</sup> Institut für Geologie und Mineralogie, Zùlpicher Str. 49b, D-50674 Köln, Germany

<sup>b</sup> Dipartimento di Scienze della Terra, Università degli Studi di Firenze, via G. la Pira 4, I-50121, Firenze, Italy

<sup>c</sup> Isotope Geosciences, Scottish Universities Environmental Research Centre, East Kilbride G75 0QF, UK

## ARTICLE INFO

### Article history:

Received 23 April 2021

Received in revised form 8 March 2022

Accepted 16 March 2022

Available online 20 April 2022

Editor: R. Dasgupta

### Keywords:

<sup>182</sup>W

intraplate volcanism

mantle plumes

mantle geodynamics

short-lived isotopes

## ABSTRACT

Several studies have revealed small heterogeneities in the relative abundance of <sup>182</sup>W, the radiogenic nuclide of short-lived <sup>182</sup>Hf ( $t_{1/2} = \sim 9$  Ma), in terrestrial rocks. Whereas the majority of Archean rocks display <sup>182</sup>W excesses relative to bulk silicate Earth, many young ocean island basalts show small <sup>182</sup>W deficits, in particular if they are sourced from deep-rooted mantle plumes. The origin of this anomaly is still ambiguous, proposed models focus on core-mantle interaction or the presence of reservoirs in the lower mantle that have been isolated since the Hadean. In order to evaluate the role of upper mantle reservoirs, we report the first <sup>182</sup>W data for intraplate basalts where a deep plume origin is still debated (Ascension Island, Massif Central, Siebengebirge and Eifel) and intraplate volcanic rocks associated with either plume or subduction zone environments (Italian Magmatic Provinces) and compare them to new data for basalts that have a deep mantle plume origin (La Réunion and Baffin Island). The proto-Iceland plume basalts from Baffin Island have uniform and modern mantle-like  $\mu^{182}\text{W}$  of around 0 despite extremely high (<sup>3</sup>He/<sup>4</sup>He). In contrast, basalts from both volcanic edifices from La Réunion span a range from modern upper mantle values to deficits as low as  $\mu^{182}\text{W} = -8.8$  ppm, indicating a heterogeneous source reservoir. The  $\mu^{182}\text{W}$  in all other intraplate volcanic provinces overlap the composition of modern upper mantle to within 3 ppm. The absence of resolvable <sup>182</sup>W anomalies in these intraplate basalts, which partially tap the lithospheric mantle, suggests that primordial components are neither present in the central and southern European lithosphere nor in the European asthenospheric reservoir (EAR). The general absence of <sup>182</sup>W anomalies in European plume-related basalts can either be explained by a shallow mantle source or by the absence of isotopically anomalous and isolated domains in the deep mantle beneath the northern hemisphere, as also suggested by geophysical evidence.

© 2022 The Author(s). Published by Elsevier B.V. This is an open access article under the CC BY-NC-ND license (<http://creativecommons.org/licenses/by-nc-nd/4.0/>).

## 1. Introduction

Tungsten isotope measurements of Archean rocks (e.g., Willbold et al., 2011; Puchtel et al., 2016; Rizo et al., 2016; Tusch et al., 2019, 2021a, 2021b) and modern plume-derived basalts (e.g., Willbold et al., 2011; Rizo et al., 2016; Mundl et al., 2017; Mundl-Petermeier et al., 2019, 2020) have revealed heterogeneities in the relative abundance of <sup>182</sup>W, the radiogenic nuclide of short-lived <sup>182</sup>Hf with a half-life of  $\sim 9$  Ma (Vockenhuber et al., 2004). The presence of <sup>182</sup>W anomalies in modern basalts requires the preservation of old mantle domains that either formed by early crystal-liquid fractionation within the silicate Earth (Touboul et al.,

2012; Tusch et al., 2021a) or did not fully equilibrate with material the Earth received during its late accretion (e.g., Willbold et al., 2011; Tusch et al., 2021b). Both theories are consistent with observations from other short-lived decay series, such as <sup>146</sup>Sm-<sup>142</sup>Nd or <sup>129</sup>I-<sup>129</sup>Xe that indicate early crystal-liquid fractionation within the silicate Earth (Carlson and Boyet, 2008; Peters et al., 2018) and the survival of primordial, relatively undegassed domains deep in the mantle (e.g., Mukhopadhyay, 2012).

In contrast to most Archean rocks, modern intraplate basalt provinces display deficits in <sup>182</sup>W (e.g., Mundl et al., 2017; Mundl-Petermeier et al., 2019, 2020). Positive <sup>182</sup>W isotope compositions in modern rocks have so far only been reported for basalts from the proto-Iceland plume and the Ontong-Java-Plateau (Rizo et al., 2016). <sup>182</sup>W deficits in modern ocean island basalts (OIBs) are consistent with the preservation of a residual basal magma ocean domain that equilibrated with the core (e.g., Mundl-Petermeier et al.,

\* Corresponding author.

E-mail address: [mike.jansen@uni-koeln.de](mailto:mike.jansen@uni-koeln.de) (M.W. Jansen).

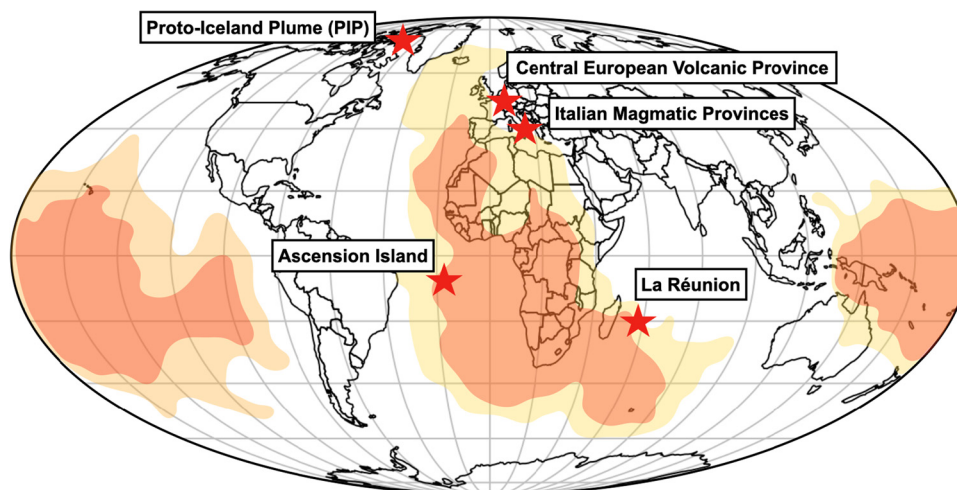


**Fig. 1.** Location of the volcanic settings investigated. The background map is modified after French and Romanowicz (2015) and includes the inferred location of LLSVPs and ULVZs based on the whole-mantle-shear-wave velocity model SEMUCB-WM1. LLSVP boundaries are marked by yellow color shadings, center regions are marked in red. (For interpretation of the colors in the figure(s), the reader is referred to the web version of this article.)

2019, 2020), or the presence of mantle reservoirs formed by continuous core-mantle interaction (e.g., Rizo et al., 2019 and references therein). Seismic constraints reveal a spatial association between mantle plumes and zones of reduced shear-velocity, termed Large Low Shear Velocity Provinces (LLSVPs) and Ultra Low Velocity Zones (ULVZs) (French and Romanowicz, 2015). These zones are possibly home to long-term isolated, primordial domains at the core-mantle boundary (e.g., French and Romanowicz, 2015; Rizo et al., 2016; Mundl et al., 2017; Mundl-Petermeier et al., 2020, 2019).

Previous W isotope studies have primarily focused on OIBs that likely originated from deep-rooted mantle plumes, as revealed by shear-wave velocity models (e.g., French and Romanowicz, 2015). These groups of “continuous plumes”, which extend throughout the whole mantle, are the most promising source of deep mantle that would record interaction with the core. Notably, only two samples of mid ocean ridge basalts (MORB) have been analyzed thus far (e.g., Mundl et al., 2017; Rizo et al., 2019). Therefore, the composition of the convecting upper mantle remains largely unknown.

Despite the assumption of whole mantle convection and mantle depletion as a consequence of crust formation, numerous studies on long-lived radiogenic isotope compositions have demonstrated that the upper mantle contains innumerable geochemical heterogeneities formed by crustal recycling (e.g., Hart et al., 1992; Regelous et al., 2009; Paulick et al., 2010). Early geochemical models suggested that the composition of some OIBs can be best explained by the presence of recycled enriched material in the lower mantle (Hart et al., 1992). However, this view was recently questioned by seismic evidence that found no detectable upwelling of lower mantle material at plume-related settings that are characterized by OIBs with an enriched composition (e.g., French and Romanowicz, 2015; Jackson et al., 2020). To resolve this ambiguity, upper mantle material, such as refertilized subcontinental lithospheric mantle (SCLM) (e.g., Lustrino and Wilson, 2007), recycled plume material (e.g., Hoernle et al., 1995) or delaminated, ancient crustal components were suggested as alternative sources for the enriched geochemical composition of some intraplate basalts (e.g., Regelous et al., 2009). However, the contributions of these different upper-mantle sources to the  $^{182}\text{W}$  inventory of intraplate basalts are still poorly constrained. Currently, there are only  $^{182}\text{W}$  data for two MORBs (Mundl et al., 2017; Rizo et al., 2019) and two contrasting datasets for kimberlites (Tappe et al., 2020; Nakanishi et al., 2021). Kimberlites may either record the composition of the upper mantle (Tappe et al., 2020) or of lower mantle reservoirs

(Nakanishi et al., 2021). Thus, it is presently unknown if  $^{182}\text{W}$  heterogeneities are also preserved in upper mantle domains or if they are exclusively present in lower mantle domains.

To better constrain the W isotope compositions of upper-mantle domains we have analyzed a comprehensive suite of continental- and oceanic intraplate basalts from a variety of tectono-magmatic settings. This group of samples comprises oceanic intraplate basalts from Ascension Island as well as continental intraplate settings, including the European Cenozoic Volcanic Province (CEVP) (Eifel, Massif Central, Siebengebirge) and intraplate basalts from the Italian Magmatic Province (IMP) (Mt. Etna, Hyblean Plateau, Pantelleria). The intraplate basalts from the IMP are compared to volcanic rocks linked to a nearby subduction zone environment (Stromboli, Vulture, Vesuvio). Our sample set is complemented by deep mantle plume-derived basalts that originate from the Piton des Neiges (PDN) and Piton de la Fournaise (PDF) volcanic edifices at La Réunion (Kurzweil et al., 2019) and high  $^3\text{He}/^4\text{He}$  basalts from the proto-Iceland plume (PIP) from Baffin Island (Stuart et al., 2003; Starkey et al., 2009). To reconstruct the mantle sources involved and to explore the long-term preservation potential of upper mantle reservoirs, we combine new high precision W-Hf-Nd isotope data and W-U-Th concentration data with previously published Sr-Nd-Pb-He and some new Hf-Nd isotope data.

## 2. Sample material

For this study we have selected 46 samples, including basalts, basanites and melilitites ( $\text{SiO}_2 = 38.9 - 52.63$  wt.%;  $\text{MgO} = 4.47 - 20.0$  wt.%, Table A-1) from different geodynamic settings (Fig. 1). With the exception of samples from the Eifel, Massif Central, and the Hyblean Plateau, all samples have been subject to detailed geochemical investigation. For sources of additional data see supplementary tables A-1 to A-4. If not already published, existing Hf-Nd isotope data and W-U-Th concentration data have been complemented herein.

## 3. Analytical methods

### 3.1. Isotope dilution and long-lived radiogenic isotope measurements

High-precision determinations of W, U, Th and Ta concentrations were performed by isotope dilution, together with  $^{176}\text{Hf}/^{177}\text{Hf}$  and  $^{143}\text{Nd}/^{144}\text{Nd}$  isotope measurements. While  $^{182}\text{W}$  was analyzed for all samples,  $^{176}\text{Hf}/^{177}\text{Hf}$  and  $^{143}\text{Nd}/^{144}\text{Nd}$  have only

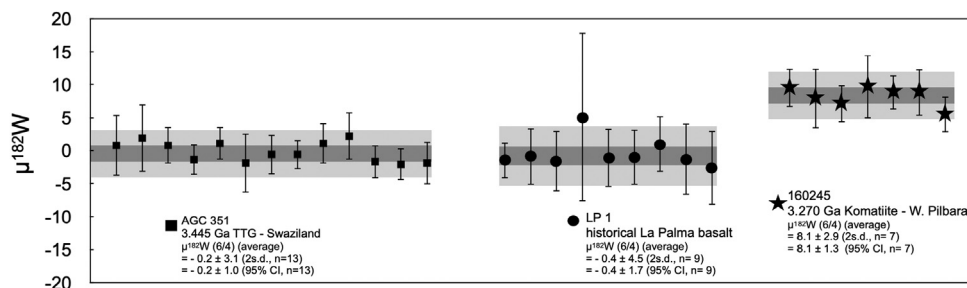


**Fig. 2.** Intermediate precision for  $\mu^{182}\text{W}$  (6/4). Values are inferred from the repeated analysis of multiple digestions for our in-house reference materials granite AGC 351, basalt LP 1 and komatiite 160245 that are reported relative to NIST SRM 3163. Each symbol refers to the average value of multiple measurements (up to  $n = 14$ ) conducted during an analytical session. The uncertainties for the session mean values are given by the corresponding 95% c.i. The long-term intermediate precisions (2 standard deviations) for our in-house reference materials are given by the 2 SD of the session mean values.

been determined on samples where data were not available. Isotope dilution measurements for W, U, Th and Ta have only been conducted for samples where trace element measurements yielded concentrations  $\leq 600$  ng/g. For higher concentrations conventional quadrupole ICPMS data were used. A detailed description of the analytical procedure for the measurements of long-lived radiogenic isotopes as well as major and trace element concentrations can be found in the Appendix.

### 3.2. Tungsten isotope measurements

Tungsten was separated from bulk rock samples following the protocols described in Tusch et al. (2019, 2021a, 2021b), applying a four-column procedure employing cation, anion, TEVA and TODGA resins. Depending on the W concentration, up to 30 sample splits (1–1.2 g) were individually passed through the chemical separation procedure and recombined prior to the measurement. The approximate amount of sample material used to generate the measurements is reported in Table 2. Procedural yields for W were generally  $\geq 70\%$ . Total procedural W blanks were determined by isotope dilution (i.e. Kurzweil et al., 2018) and were usually below 300 pg, contributing less than 1% to the total analyte. High-precision W isotope composition measurements were performed using the Thermo-Fisher® Neptune Plus MC-ICP-MS at the University of Cologne, following the protocols given by Tusch et al. (2019, 2021a, 2021b). To assess the long-term reproducibility we always included one of our three in-house reference materials during each analytical session (historical La Palma Basalt “LP 1”, Kurzweil et al. (2019) and a 3455 Ma old grey gneiss “AGC 351” from southwest Swaziland Kröner et al. (2014)). During the analytical campaign we also analyzed a 3.27 Ga old komatiite from the Pilbara Craton (sample 160245, Ruth Well Formation), Western Australia, that was shown to exhibit an excess in  $\mu^{182}\text{W}$  of  $+6.8 \pm 2.3$  ppm (Tusch et al., 2021a,b). Final results are reported in the  $\mu$  notation (ppm deviation relative to NIST SRM 3163). The intermediate precision of our in-house reference materials, given by the mean value of multiple session averages, is  $\mu^{182}\text{W} = -0.2 \pm 1.0$  ppm (AGC 351),  $-0.7 \pm 1.2$  ppm (LP 1) and  $8.1 \pm 1.3$  ppm (160245), respectively (Fig. 2). It must be noted that some samples were measured during the early campaign of the Tusch et al. (2019) study and bear small nuclear field shift effects on  $^{183}\text{W}$  (marked in Table 2). These effects were shown to become negligible after applying a modified dry-down protocol ( $\text{cHNO}_3 - 30\% \text{H}_2\text{O}_2$ ) (Tusch et al., 2019). However, nuclear field shift effects do not affect  $^{182}\text{W}$  compositions that are mass bias corrected relative to  $^{186}\text{W}/^{184}\text{W}$  ( $^{182}\text{W}$  (6/4)) and do not involve  $^{183}\text{W}$ . This is demonstrated by our data for sample Ei 27, that involve both dry-down protocols and yield  $^{182}\text{W}$  (6/4) isotope compositions that overlap within error (Table 2). A more detailed description of analytical methods can be found in the supplementary material.

## 4. Results

Major and trace element compositions are reported in supplementary Table A-1 and  $^{143}\text{Nd}/^{144}\text{Nd}$  and  $^{176}\text{Hf}/^{177}\text{Hf}$  compositions are presented in Table A-5. Values of  $\epsilon\text{Nd}$  ( $-3.0$  to  $+9.1$ ) and  $\epsilon\text{Hf}$  ( $-3.7$  to  $+17.5$ , Table A-5, Fig. 3) show a broad range of different mantle-reservoir compositions (Fig. 3) (e.g., Hofmann, 2003). Concentrations of W, U and Th are reported in Table 1. Tungsten concentrations range from 50 ng/g (DUR 7) to 6770 ng/g (VES 95). Most samples compositionally overlap the inferred W/Th and W/U of modern MORBs and OIBs (e.g., König et al., 2008, 2011) (Fig. 4). However, extremely elevated W/Th ratios were found in ASD 16 from Ascension Island ( $\text{W}/\text{Th} = 5.86$ ) and DUR 1 from Baffin Island ( $\text{W}/\text{Th} = 16.5$ ), which are further discussed below. The session averages for high-precision W isotope analysis together with their corresponding 95% CI are reported in Table 2. Tables A-2 and A-3 provide an overview of single W isotope measurement runs for all session averages. Our samples exhibit  $\mu^{182}\text{W}$  values between  $-8.8 \pm 4.1$  ppm and  $+3.9 \pm 4.0$  ppm, within the range of previously reported  $^{182}\text{W}$  compositions of MORBs and OIBs (Fig. 5; e.g., Rizo et al., 2019; Mundl-Petermeier et al., 2019, 2020). Clearly resolvable negative  $\mu^{182}\text{W}$  values are only found for the PDF volcanic edifice at La Réunion.

## 5. Discussion

### 5.1. Characterization of mantle domains using $^{143}\text{Nd}/^{144}\text{Nd}$ and $^{176}\text{Hf}/^{177}\text{Hf}$ compositions

Based on long-lived (e.g., Sr-Nd-Hf-Os), short-lived (e.g.,  $^{142}\text{Nd}$ ,  $^{182}\text{W}$ ) radiogenic isotope and noble gas compositions (e.g.,  $^3\text{He}/^4\text{He}$ ), it has been suggested that intraplate volcanism taps an array of chemically distinct reservoirs in the mantle (e.g., Hofmann, 2003). This array is commonly characterized by different mantle endmembers displaying moderately radiogenic (PREMA, FOZO) or un-radiogenic  $^{143}\text{Nd}/^{144}\text{Nd}$  and  $^{177}\text{Hf}/^{176}\text{Hf}$  (EM I, EM II) as well as highly radiogenic Pb-isotope compositions (HIMU) (e.g., Hofmann, 2003 and references therein). The convecting upper mantle tapped by MORB has highly radiogenic  $^{143}\text{Nd}/^{144}\text{Nd}$  and  $^{177}\text{Hf}/^{176}\text{Hf}$  that likely represents the depleted residue after crust formation (e.g., Hofmann, 2003; Hart et al., 1992). Another component has been identified that shows distinctly higher  $^3\text{He}/^4\text{He}$  ratios than average upper mantle components ( $^3\text{He}/^4\text{He} = \sim 8 \text{R}/\text{R}_A$ ) (e.g., Hart et al., 1992; Hofmann, 2003 and references therein). While earlier studies defined a common deep mantle endmember composition that resembles a less-degassed, primordial reservoir (FOZO) (e.g., Hart et al., 1992), the compositional spread of associated Sr-Nd-Hf-Pb isotope data questions the presence of such a distinct endmember (e.g., Starkey et al., 2009). This is further strengthened by recent studies of Mundl-Petermeier et al. (2020) and Jackson et al. (2020)

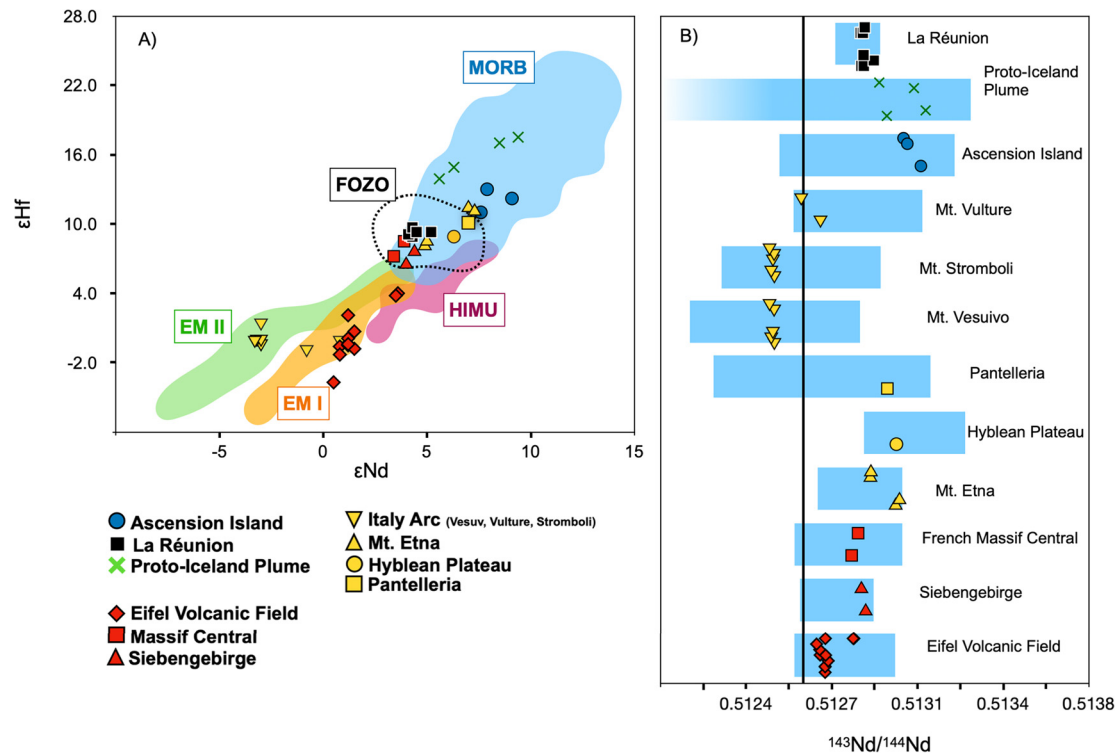


**Fig. 3.**  $\epsilon_{\text{Hf}}$  vs.  $\epsilon_{\text{Nd}}$  compositions of all analyzed basalts relative to compositional fields for classical mantle domains (A) and comparison of  $^{143}\text{Nd}/^{144}\text{Nd}$  with literature data (B). In Fig. 3A, the sample selection covers most traditional mantle endmembers and our data are in good agreement with previously reported data in the literature. Color shaded fields indicate compositional variations of MORBs, OIBs and intraplate volcanic rocks. In Fig. 3B,  $^{143}\text{Nd}/^{144}\text{Nd}$  data of our samples are compared to previously published data. The blue shaded areas thereby indicate the total range of published data. For further references see the supplementary information. CHUR values from Bouvier et al. (2008). Compositional fields were generated using data from the GeoRoc Database (<http://georoc.mpch-mainz.gwdg.de/georoc/>).

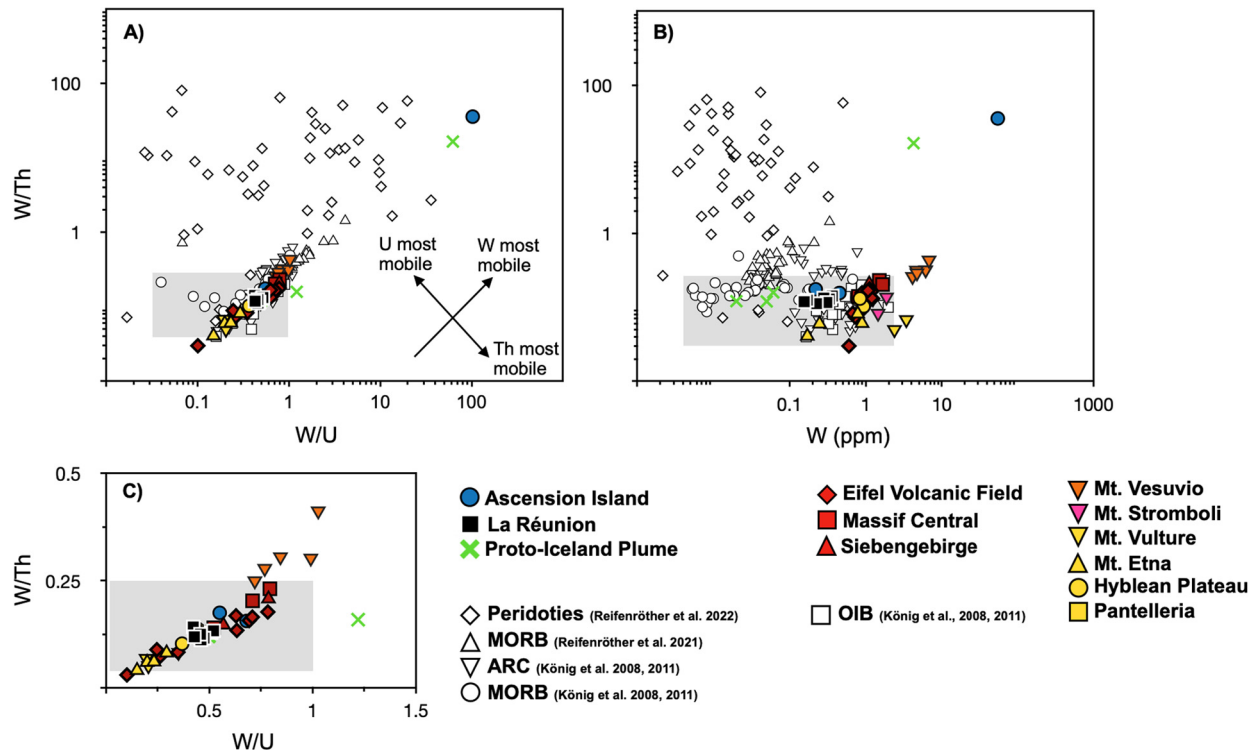


**Fig. 4.** Evaluation of elemental W behavior based on W/Th vs. W/U (A, C) and W/Th vs. W (B) patterns. Most samples analyzed throughout this study overlap with the inferred canonical field as defined by MORB and OIB, indicating a control of igneous processes on elemental W systematics. Many arc-related samples from Italy (Mt Stromboli and Mt. Vulture) do not display significantly elevated elemental W/Th and W/U ratios. Only samples from Mt. Vesuvio are displaced towards higher W/Th ratios. Some samples from the Italian Magmatic Provinces, Ascension Island and the Proto-Iceland plume display selective W enrichments and elevated W/Th ratios. This is in good agreement with secondary re-distribution of W during alteration and within aqueous subduction zone environments. Grey shaded areas define canonical compositions of MORB, OIB previously analyzed by König et al. (2008, 2011). Data from König et al. (2008, 2011) and Reifenröther et al. (2021, 2022) are plotted for comparison.



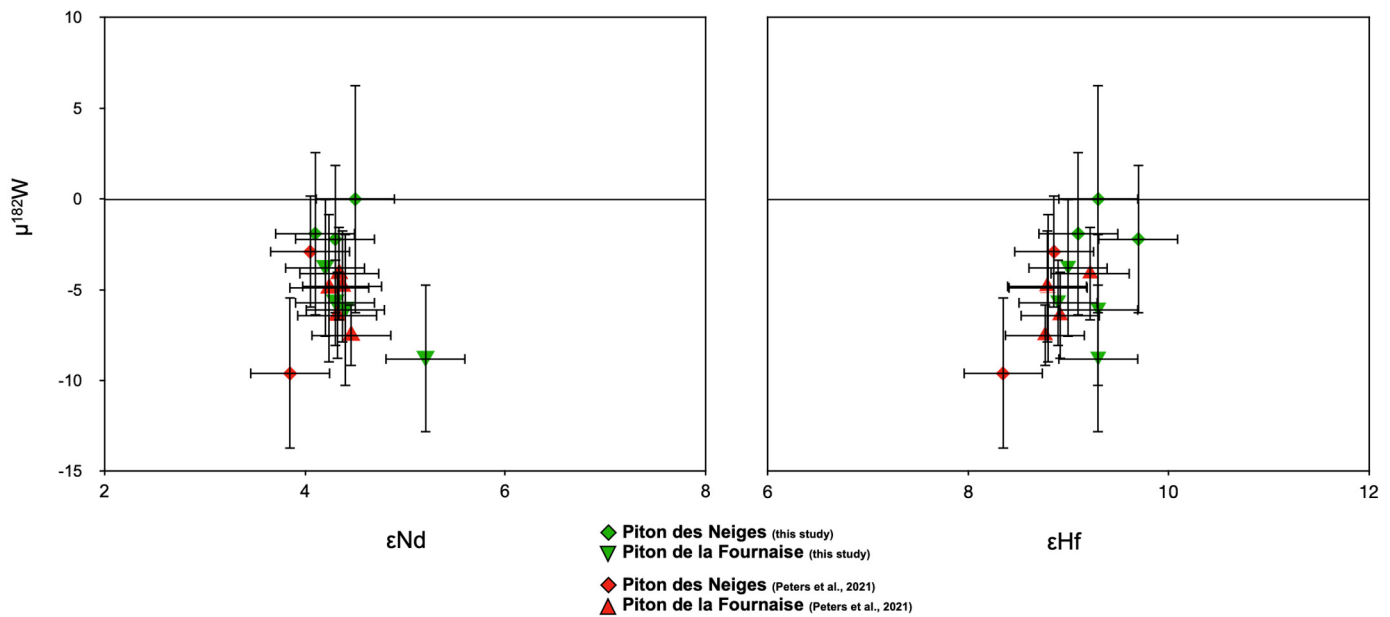


**Fig. 5.**  $^{182}\text{W}$  vs.  $^{143}\text{Nd}/^{144}\text{Nd}$  and  $^{182}\text{W}$  vs.  $^{176}\text{Hf}/^{177}\text{Hf}$  compositions of La Réunion samples from this study and Peters et al. (2021). Samples of both studies largely overlap within their  $^{143}\text{Nd}/^{144}\text{Nd}$  and  $^{176}\text{Hf}/^{177}\text{Hf}$  isotope compositions but display heterogeneous  $^{182}\text{W}$  isotope compositions.

who have identified different co-variations between  $^3\text{He}/^4\text{He}$  ratios and  $^{182}\text{W}$  isotope compositions in modern OIBs that indicate a variety of undegassed mantle endmember compositions. While it was long believed that recycled materials only contribute to deep-rooted plumes from the lower-mantle, recently published studies on intraplate volcanic rocks by Belay et al. (2019) and Guimarães et al. (2020) have invoked delaminated and refertilized SCLM materials as sources for OIB-like volcanism in places where a plume is difficult to resolve. This is broadly similar to models for the origin of the DUPAL-anomaly (Dupré and Allègre, 1983) found in volcanic rocks from the southern hemisphere (Hart et al., 1992). It is identified by distinct  $^{207,208}\text{Pb}/^{204}\text{Pb}$  and  $^{87}\text{Sr}/^{86}\text{Sr}$  patterns, and is thought to originate from disrupted continental crust and SCLM material recycled into the upper-mantle (e.g., Regelous et al., 2009).

Considering the geodynamic settings covered by this study, the large range of  $\varepsilon\text{Nd}$  (−3.0 to +9.1) and  $\varepsilon\text{Hf}$  compositions (−3.7 to +17.5, Table A-5, Fig. 3) of the samples investigated resemble a broad range of mantle endmember compositions, classically displayed by plume-sourced OIBs. Plume-related basalts from La Réunion and the PIP display a limited compositional range, overlapping with FOZO (La Réunion:  $\varepsilon\text{Nd} = +4.1$  to  $+4.5$ ;  $\varepsilon\text{Hf} = +8.9$  to  $+9.7$ ) and enriched MORB (PIP:  $\varepsilon\text{Nd} = +5.6$  to  $+9.4$ ;  $\varepsilon\text{Hf} = +14.9$  to  $+17.5$ ). In contrast, a plume origin for settings like the CEVP, the IMP and Ascension Island has been proposed, but is still under debate (e.g., Granet et al., 1995; French and Romanowicz, 2015). The samples analyzed here resemble EM I/EM II to HIMU compositions (EVF:  $\varepsilon\text{Nd} = +0.8$  to  $+3.6$  and  $\varepsilon\text{Hf} = -1.3$  to  $+4.0$ ), FOZO (Massif Central, Siebengebirge, Pantelleria, Mt. Etna, Hyblean Plateau:  $\varepsilon\text{Nd} = +3.4$  to  $+7.0$ ;  $\varepsilon\text{Hf} = +6.5$  to  $+10.1$ ) and enriched MORB (Ascension Island:  $\varepsilon\text{Nd} = +7.6$  to  $+9.1$ ;  $\varepsilon\text{Hf} = +11.0$  to  $+13.0$ ) (Fig. 3). As expected, the subduction related samples from the IMP display evidence for the contribution of recycled crustal materials to their sources ( $\varepsilon\text{Nd} = -3.0$  to  $+0.8$ ;  $\varepsilon\text{Hf} = -1.0$  to  $+2.8$ ) (Table A-5, Fig. 3).

## 5.2. Elemental W-Th-U systematics and sources of W

In silicate systems, W is one of the most incompatible elements, similar to U and Th. Due to the moderately siderophile and fluid mobile behavior of W, elemental ratios of W and lithophile

elements like U and Th can provide valuable insights on the behavior of W in modern igneous reservoirs (e.g., König et al., 2008, 2011; Kurzweil et al., 2019; Newsom et al., 1996; Noll et al., 1996). Detailed investigation of MORBs and OIBs by König et al. (2008, 2011) showed a discrete range of “canonical” elemental W/Th ratios (MORB: W/Th = 0.090 – 0.24 / OIB: W/Th = 0.040 – 0.23), implying that this element ratio is solely controlled by crystal-liquid fractionation in silicate systems, where W-Th-U are so incompatible that partial melting does not significantly fractionate W/Th and W/U ratios. In contrast, W concentrations and related W/Th and W/U ratios in arc lavas and altered samples can be substantially elevated due to the selective re-distribution of W in fluid-mediated environments (e.g., König et al., 2008, 2011; Reifenröther et al., 2021, 2022). As secondary W re-distribution can overprint primary  $^{182}\text{W}$  isotope signatures, it is essential to carefully monitor the elemental W budget of samples prior to  $^{182}\text{W}$  isotope analysis (e.g., Tusch et al., 2021a,b).

Considering that most samples analyzed here have W/Th and W/U ratios similar to the canonical range defined by MORB and OIB (Fig. 4), we regard their W budget as undisturbed by metasomatic processes. However, samples from Ascension Island (ASD 16) and the proto-Iceland plume (DUR 1) exhibit significantly elevated W concentrations of 55.2 ppm (ASD 16) and 4.24 ppm (DUR 1) at high W/Th ratios (16.5, DUR 1; 35.6, ASD 16). While such extreme enrichments could be caused by contamination during sample preparation (e.g., saw blade/jaw-crusher), both samples lack significant enrichments of other siderophile elements such as Ni, Cr or Fe. Despite the lack of alteration signatures in other sensitive isotope (e.g.,  $^{87}\text{Sr}/^{86}\text{Sr}$  (Stuart et al., 2003; Starkey et al., 2009; Paulick et al., 2010) and trace element markers (e.g., Ba), this extreme enrichment of W might therefore be caused by fluid-controlled alteration processes that selectively mobilized W. This is consistent with previous studies by Kurzweil et al. (2020) reporting substantially elevated W concentrations and related W/Th, W/U ratios in Eoarchean rocks from Isua, suggesting the preferential mobilization of W within  $\text{CO}_2$  rich fluids. Among the samples analyzed here, sample ASD 16 has been collected from the submarine ASI #3 drillcore, which was likely disturbed by hydrothermal alteration (e.g., Nielson and Sibbett, 1996). High W/Th of sample DUR 1 may reflect surface alteration, with fluids likely being re-

**Table 1**

Concentrations of W, U, Th and related elemental W/Th, W/U ratios. With the exception of samples from the Eifel Volcanic Field, Siebengebirge and sample ZM 12 (Massif Central), all concentrations were obtained by high precision measurements.

Sample	W ( $\mu\text{g/g}$ )	Th ( $\mu\text{g/g}$ )	U ( $\mu\text{g/g}$ )	W/Th	W/U
<b>La Réunion</b>					
REU 1	0.363	2.56	0.860	0.142	0.422
REU 11	0.331	2.57	0.650	0.129	0.509
REU 13	0.281	2.11	0.540	0.133	0.520
REU 17	0.308	2.65	0.650	0.116	0.474
REU 18	0.225	2.01	0.490	0.112	0.459
REU 19	0.170	1.36	0.371	0.125	0.457
REU 20	0.155	1.30	0.363	0.119	0.427
<b>Mt. Etna</b>					
ET 1	0.171	4.13	1.14	0.041	0.150
ET 2	0.247	4.13	1.24	0.0598	0.199
ET 3	0.893	14.68	3.85	0.0608	0.232
ET 4	0.783	9.59	2.67	0.082	0.293
<b>Hyblean Plateau</b>					
IBL 1	0.937	9.13	2.55	0.103	0.368
IBL 2	0.837	6.39	1.69	0.131	0.495
<b>Eifel Volcanic Field</b>					
Ei 2	1.12	6.32	1.43	0.177	0.783
Ei 4	1.23	9.39	2.71	0.131	0.454
Ei 9	0.893	5.70	1.29	0.157	0.693
Ei 10b	0.601	19.8	5.93	0.0303	0.101
Ei 12	0.727	9.82	2.77	0.0740	0.263
Ei 16b	1.197	7.26	1.69	0.165	0.708
Ei 22	0.675	8.18	1.94	0.0825	0.348
Ei 25	1.196	8.93	1.89	0.134	0.633
Ei 27	0.870	9.73	3.54	0.0894	0.246
Ei 29	1.23	8.10	2.07	0.152	0.594
Ei 32	1.07	6.38	1.70	0.168	0.629
<b>Siebengebirge</b>					
SG 19	1.11	5.33	1.41	0.208	0.786
SG 30	1.02	6.95	1.80	0.147	0.568
<b>Massif Central</b>					
ZM 10	1.506	6.53	1.90	0.231	0.793
ZM 12	1.66	8.17	2.34	0.203	0.709
ZM 14	0.798	5.71	1.53	0.140	0.521
<b>Proto-Iceland Plume</b>					
PAD 6	0.061	0.383	0.0500	0.159	1.220
PAD 8	0.020	0.165	0.0400	0.121	0.498
DUR 1	4.246	0.258	0.0680	16.5	62.4
DUR 7	0.050	0.415	0.101	0.120	0.495
<b>Ascension Island</b>					
MAR 4	0.220	1.26	0.400	0.175	0.550
ASI 3	0.451	2.89	0.663	0.156	0.680
ASD 16	55.2	1.55	0.537	35.6	103
<b>Mt. Vesuvio</b>					
VES 01	4.11	16.8	5.71	0.245	0.720
VES 07	6.12	20.3	7.2	0.301	0.844
VES 16	4.62	15.5	4.7	0.298	0.991
VES 95	6.77	16.6	6.59	0.408	1.027
VES 97	4.70	17.1	6.12	0.274	0.768
<b>Pantelleria</b>					
PAN 5	0.816	6.12	1.85	0.133	0.441
<b>Mt. Stromboli</b>					
STR 07	1.87	14.5	3.89	0.129	0.481
STR 50	1.45	18.5	4.13	0.078	0.351
<b>Mt. Vulture</b>					
VLT 14	3.41	53.6	17.6	0.0636	0.194
VLT 49	2.38	50.9	11.6	0.0468	0.205

leased from the underlying basement (e.g., Mundl-Petermeier et al., 2019).

The intraplate volcanic samples from the CEVP mostly display similar W/Th ratios in the canonical range (Fig. 4, Table 1). Only one melilitite from the Eifel exhibits a sub-canonical W/Th ratio (Ei 10b; W/Th = 0.03). The origin of melilitites is debated, but

trace element modeling and P-T estimates suggest an origin in the lowermost lithospheric mantle (e.g., Jung et al., 2011; Pfänder et al., 2018). A study by Pfänder et al. (2018) has further proposed 3–5% partial melting of a highly enriched, metasomatized carbonated phlogopite bearing garnet-lherzolite. Therefore, it is likely that some minerals such as rutile, phyllosilicates or amphibole that are stable in the lithospheric mantle may have retained some of the W during low-degree partial melting (e.g., Liu et al., 2018).

The elemental W systematics of the Italian basalts needs to be discussed in the context of a complex subduction zone setting. Whereas some subduction-related lavas from Vesuvio exhibit slightly elevated W/Th ratios, Italian arc and intraplate samples fall within the canonical range defined by MORB and OIB with some samples pointing towards subcanonical values (Mt Etna and Vulture). The origin of these low W/Th was suggested as being related to the interaction with the carbon-rich SCLM (Bragagni et al., 2022). A closer look at the W-Th-U concentrations of the subduction-related samples from Vesuvio, Vulture and Stromboli (W = 1.45 – 6.77 ppm; Th = 14.5 – 40.9 ppm; U = 3.89 – 17.9 ppm) reveals W-U-Th abundances that by far exceed previously reported concentration ranges from arc settings (König et al., 2008, 2011, Fig. 4). Avanzinelli et al. (2018) suggested the presence of a complex mantle source beneath Vesuvio, characterized by a first episode of subduction-related metasomatism due to silica-rich components (similar to those affecting Stromboli), capable of enriching the mantle in Th and other incompatible trace elements. The recent addition of carbonate-rich fluids/melts was inferred to account for  $^{238}\text{U}$ -excesses measured in Vesuvio's magmas. In this context,  $\text{CO}_2$ -rich fluids and melt-like slab components display a great potential of mobilizing W as well as U to similar extents (e.g., König et al., 2008, 2011). This is clearly illustrated in Fig. 4, where samples from Vesuvio are displaced towards higher W/Th and W/U ratios compared to our samples from Stromboli that display canonical W/Th ratios and carry no  $^{238}\text{U}$ -excess (Bragagni et al., 2014, 2022; Tommasini et al., 2007). With the exception that Stromboli basalts lack any evidence of the involvement of  $\text{CO}_2$  rich components, basalts from Stromboli and Vesuvio are geochemically similar, suggesting related mantle sources (Peccerillo, 2017).

### 5.3. Origin of W isotope compositions in the samples from deep-rooted mantle plumes

Despite a deep mantle origin (e.g., French and Romanowicz, 2015), volcanic rocks from La Réunion have previously been shown to plot within a restricted compositional range of long-lived radiogenic isotope compositions, similar to the PREMA/FOZO component with a clear DUPAL-flavor (Dupré and Allègre, 1983; Bosch et al., 2008). This composition is present in the samples analyzed within this study (Table A-5, Fig. 3). The negative  $\mu^{182}\text{W}$  found for the PDF basalts from La Réunion (as low as  $-8.8 \pm 4.4$  ppm, Table 2) are consistent with previous investigations (Rizo et al., 2019; Peters et al., 2021). Notably, samples from the older PDN edifice reveal no significant W isotope anomalies, scattering around the inferred modern upper-mantle value ( $\mu^{182}\text{W} = -2.2 \pm 4.1$  to  $+0.0 \pm 6.3$ ; Fig. 6). While such compositions might reflect heterogenous source compositions of both volcanoes, deficits as low as  $-9.6$  (Peters et al., 2021) argue for a sampling bias of volcanic edifices, PDN (N = 5) and PDF (N = 14) respectively. Rizo et al. (2019) and Peters et al. (2021) have suggested that La Réunion basalts preserve a contribution from a lower mantle reservoir that has previously interacted with the core. This is broadly similar to the model developed by Mundl-Petermeier et al. (2019, 2020) and Jackson et al. (2020) who have ascribed a negative correlation of He and W isotope compositions to the presence of primordial reservoirs that remained isolated for most of Earth history (see also Graham, 2002 for He). These authors have also proposed that these primordial

**Table 2**  
Measured tungsten isotope compositions of all investigated basalts. Samples marked with “\*” have been measured using the older protocol from Tusch et al. (2019).

Sample	$\mu^{182}\text{W}$ (6/4) ( $\pm 95\%$ CI)	$\mu^{183}\text{W}$ (6/4) ( $\pm 95\%$ CI)	$\mu^{182}\text{W}$ (6/3) ( $\pm 95\%$ CI)	$\mu^{184}\text{W}$ (6/3) ( $\pm 95\%$ CI)	$\mu^{182}\text{W}$ Corr (6/3) ( $\pm 95\%$ CI)	Sample weight (g)
<b>La Réunion</b>						
REU 1	-3.8 ± 3.8	-1.9 ± 4.2	-3.5 ± 2.9	+1.3 ± 2.8	-5.3 ± 3.6	2.5
REU 11	-6.1 ± 4.2	-0.9 ± 4.0	-4.8 ± 2.8	+0.6 ± 2.7	-5.4 ± 3.8	2.5
REU 13	-8.8 ± 4.1	-1.2 ± 3.7	-7.7 ± 2.3	+0.8 ± 2.5	-8.0 ± 3.6	3.8
REU 17	-5.7 ± 2.4	-3.0 ± 3.1	-4.4 ± 2.0	+2.0 ± 2.1	+2.0 ± 2.1	3.8
REU 18	-1.9 ± 4.5	+1.5 ± 4.6	-2.7 ± 3.1	-1.0 ± 3.1	-2.3 ± 4.5	5.1
REU 19	-2.2 ± 4.1	-1.7 ± 4.3	-4.5 ± 2.7	+1.2 ± 2.9	-5.5 ± 5.9	10.4
REU 20	+0.0 ± 6.3	-3.5 ± 7.5	+0.9 ± 4.2	+2.3 ± 5.0	-3.6 ± 9.9	10.7
<b>Mt. Etna</b>						
ET 1 (ave)	+1.4 ± 3.1					
ET 1 (1)	+1.0 ± 3.7	+5.3 ± 2.7	-1.1 ± 3.5	-3.5 ± 1.8	+1.0 ± 4.1	10.3
ET 1(2)	+1.9 ± 2.6	+2.2 ± 3.3	+0.8 ± 3.0	-1.5 ± 2.2	+2.2 ± 3.0	21.65
ET 2	+1.2 ± 4.2	+1.7 ± 3.3	-0.5 ± 3.5	-1.1 ± 2.2	+0.8 ± 4.7	
ET 3	+0.2 ± 3.0	-3.0 ± 4.6	+2.2 ± 4.9	+2.0 ± 3.1	-2.5 ± 5.1	2.3
ET 4	+2.0 ± 4.7	-2.7 ± 2.9	+1.4 ± 2.5	+1.8 ± 1.9	-1.8 ± 3.4	2.20
<b>Hyblean Plateau</b>						
IBL 1 (ave)	-2.1 ± 2.5					
IBL 1 (1)	-2.3 ± 2.6	+2.2 ± 2.4	+1.5 ± 1.6	-1.5 ± 1.6	-3.5 ± 2.1	10.43
IBL 1 (2)	-2.0 ± 2.5	-2.3 ± 1.5	-1.0 ± 1.1	+1.5 ± 1.0	-1.6 ± 2.3	10.62
IBL 2 (ave)	-2.5 ± 3.1					
IBL 2 (1)	-2.0 ± 3.2	-0.4 ± 2.5	-2.0 ± 2.2	+0.3 ± 1.7	-2.7 ± 3.9	10.3
IBL 2 (2)	-3.0 ± 3.1	-3.4 ± 3.0	-1.3 ± 1.6	+2.3 ± 2.0	-3.7 ± 3.1	10.52
<b>Eifel Volcanic Field</b>						
Ei 2*	-0.8 ± 2.6	-14.5 ± 2.5	+8.9 ± 2.5	+9.6 ± 1.7	-0.4 ± 2.9	2.1
Ei 4*	+2.8 ± 4.1	-9.6 ± 3.5	+10.1 ± 2.8	+6.4 ± 2.3	+5.8 ± 3.9	2.1
Ei 9*	-0.4 ± 3.3	-11.1 ± 3.7	+14.0 ± 3.0	+7.4 ± 2.5	-0.5 ± 3.6	2.1
Ei 10b*	+1.2 ± 4.3	-9.5 ± 2.9	+8.7 ± 3.7	+6.3 ± 1.9	+2.7 ± 5.1	2.1
Ei 12*	+3.9 ± 4.0	-9.2 ± 5.2	+10.3 ± 2.4	+6.1 ± 3.4	+5.1 ± 7.1	2.1
Ei 16b*	+1.9 ± 4.6	-15.5 ± 3.3	11.9 ± 3.4	10.3 ± 2.2	+2.7 ± 4.9	2.1
Ei 22*	-0.2 ± 5.3	-0.4 ± 4.1	-0.5 ± 4.0	+0.3 ± 2.7	-1.0 ± 6.1	2.1
Ei 25*	+1.8 ± 3.8	+2.0 ± 5.5	+1.5 ± 5.7	-1.3 ± 3.7	+3.5 ± 5.6	2.0
Ei 27 (ave)*	-1.0 ± 4.2					
Ei 27 (1)	-3.4 ± 2.3	+0.5 ± 1.7	-3.3 ± 1.9	-0.3 ± 1.1	-3.4 ± 3.2	2.1
Ei 27 (2)*	-2.9 ± 6.4	+5.0 ± 8.9	-7.1 ± 7.1	-3.3 ± 5.9	-3.7 ± 5.7	1.2
Ei 27 (3)	+3.1 ± 3.9	+2.9 ± 4.9	+1.2 ± 2.0	-1.9 ± 3.3	+3.0 ± 6.2	1.4
Ei 29*	-0.5 ± 2.1	+1.8 ± 1.5	-1.2 ± 1.9	+1.2 ± 1.0	+0.3 ± 2.7	2
Ei 32*	+0.4 ± 2.8	-0.2 ± 2.2	+0.8 ± 1.8	+0.1 ± 1.5	+0.5 ± 2.9	2
<b>Siebengebirge</b>						
SG 19	+0.1 ± 4.1	+1.0 ± 3.9	+1.4 ± 2.9	-0.7 ± 2.6	+2.1 ± 3.8	2.2
SG 30	+1.1 ± 4.1	+0.1 ± 4.3	-2.5 ± 5.2	-0.1 ± 2.9	-0.7 ± 2.8	2.1
<b>Massif Central</b>						
ZM 10	+0.0 ± 3.7	+0.4 ± 3.5	-0.9 ± 2.0	-0.3 ± 2.4	-1.0 ± 3.6	5.8
ZM 12	-1.3 ± 3.2	+0.5 ± 2.5	-1.2 ± 2.6	-0.3 ± 1.7	-0.4 ± 3.6	2.1
ZM 14	-4.4 ± 3.6	-4.3 ± 4.6	-2.1 ± 2.7	+2.9 ± 3.1	-6.4 ± 5.2	5.7
<b>Proto-Iceland Plume</b>						
PAD 6	-4.5 ± 8.7	-15.8 ± 6.6	+4.1 ± 9.3	+10.5 ± 4.4	-6.8 ± 11.1	10.9
PAD 8	+2.2 ± 6.3	-2.1 ± 9.2	+4.1 ± 7.0	+1.4 ± 6.6	+1.0 ± 10.4	11.6
DUR 1	+0.9 ± 2.0	-0.6 ± 1.5	+1.0 ± 1.8	+0.4 ± 1.0	-0.6 ± 1.9	1.2
DUR 7	+1.2 ± 6.8	-6.2 ± 7.0	+5.5 ± 2.5	+4.1 ± 4.7	+3.2 ± 5.2	12.2
<b>Ascension Island</b>						
MAR 4	+0.1 ± 4.7	-2.0 ± 3.6	+2.5 ± 4.3	+1.3 ± 2.4	+0.8 ± 5.2	5.2
ASI 3	-0.2 ± 3.5	-3.6 ± 3.1	+3.2 ± 3.1	+2.4 ± 2.1	-0.2 ± 3.4	3.2
ASD 16	+0.5 ± 1.8	-0.7 ± 1.0	+1.3 ± 1.4	+0.5 ± 0.7	+1.7 ± 1.6	7.2
<b>Mt. Vesuvio</b>						
VES 01 (ave)	-2.0 ± 2.5					
VES 01	-1.3 ± 3.2	+2.0 ± 1.9	-3.2 ± 2.2	-1.4 ± 1.2	-2.0 ± 2.9	1.2
VES 01 (2)	-2.8 ± 1.9	-1.4 ± 2.3	-2.0 ± 1.0	+0.9 ± 1.6	-2.5 ± 2.6	1.6
VES 07	+0.2 ± 2.6	+1.0 ± 1.8	-1.4 ± 1.7	-0.7 ± 1.2	-0.9 ± 2.6	1.5
VES 16	-3.1 ± 2.7	-1.0 ± 2.6	-2.6 ± 2.1	+0.7 ± 1.8	-3.3 ± 2.8	1.8
VES 95 (ave)	-4.5 ± 2.9					
VES 95	-5.3 ± 2.7	-1.8 ± 2.4	-3.6 ± 2.2	+1.2 ± 1.6	-4.2 ± 2.8	1.1
VES 95 (2)	-3.8 ± 3.1	-0.8 ± 2.3	-2.3 ± 2.3	+0.5 ± 1.5	-2.9 ± 3.2	1.4
VES 97	-1.6 ± 1.5	+0.6 ± 2.0	-2.3 ± 2.0	-0.4 ± 1.4	-2.0 ± 2.2	1.1
<b>Pantelleria</b>						
PAN 5	-1.4 ± 3.6	+0.6 ± 2.9	-2.7 ± 2.3	-0.4 ± 1.9	-1.8 ± 3.9	3.1
<b>Mt. Stromboli</b>						
STR 07L	+0.1 ± 2.6	-2.2 ± 2.4	+1.1 ± 2.0	+1.5 ± 1.6	-0.4 ± 3.0	2.1
STR 50	-2.2 ± 3.4	-1.9 ± 2.6	-2.4 ± 3.6	+1.3 ± 1.7	-4.5 ± 3.1	1.1
<b>Mt. Vulture</b>						
VLT 14	-1.5 ± 1.9	+0.7 ± 1.3	-2.0 ± 1.0	-0.4 ± 0.9	-1.2 ± 1.7	1.1
VLT 49	+0.4 ± 2.9	+2.8 ± 2.3	-0.7 ± 2.5	-1.9 ± 1.6	+1.0 ± 3.0	1.1

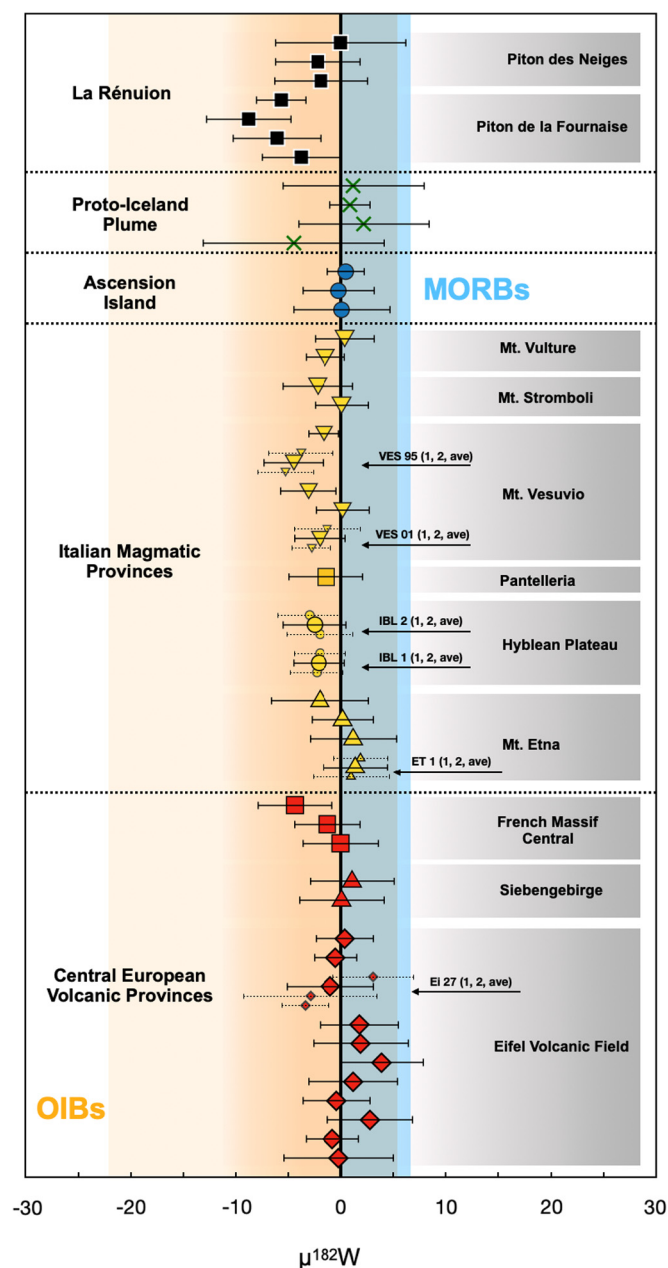


**Fig. 6.** Measured  $\mu^{182}\text{W}$  of samples investigated throughout this study. Samples from the CEVP, Ascension Island, Pantelleria and the NAIP display no anomalous  $^{182}\text{W}$  isotope compositions. In comparison, data from La Réunion indicate a heterogeneous plume source composition. The light brown colored field indicates the total range of  $^{182}\text{W}$  compositions in modern OIB (Willbold et al., 2011; Mundl et al., 2017; Rizo et al., 2019; Mundl-Petermeier et al., 2019, 2020). The light blue colored field indicates the total range of  $^{182}\text{W}$  compositions of MORBs (Mundl et al., 2017; Rizo et al., 2019).

reservoirs originate from LLSVPs, because such domains presumably formed during early silicate differentiation (high  $^3\text{He}/^4\text{He}$  ratios and  $\mu^{182}\text{W} = \sim 0$ ), and from ULVZs that may have inherited their W inventory via chemical and isotopic equilibration from the core (Mundl-Petermeier et al., 2019, 2020; Rizo et al., 2019). Assuming  $^3\text{He}/^4\text{He}$  of 13  $R_A$  (e.g. Füri et al., 2011) and  $\mu^{182}\text{W} = 0.0$  to  $-16.5$  (Rizo et al., 2019; Peters et al., 2021; this study), La Réunion lavas plot on the W-He trends that are defined by Hawaii and Samoa (e.g., Mundl-Petermeier et al., 2020). Unlike for  $^{182}\text{W}$ ,  $^{142}\text{Nd}$  heterogeneities in La Réunion lavas clearly suggest the involvement of early differentiated silicate reservoirs (Peters et al., 2018, 2021) that must have remained isolated since the late Hadean. This is in

good agreement with long-lived radiogenic isotope compositions that indicate a major contribution of the relatively unprocessed FOZO/PREMA mantle reservoir (e.g., Bosch et al., 2008). However, small-scale variations in  $^{206}\text{Pb}$ ,  $^{207}\text{Pb}$ ,  $^{208}\text{Pb}$  and  $^{143}\text{Nd}$ - $^{176}\text{Hf}$  have revealed discrete mixing relationships, suggesting that the edifices originate from compositionally distinct small-scale mantle-blobs that interacted with recycled domains and depleted mantle materials (e.g., Bosch et al., 2008).

Compiling available  $^{182}\text{W}$ ,  $^{143}\text{Nd}/^{144}\text{Nd}$  and  $^{176}\text{Hf}/^{177}\text{Hf}$  data for the La Réunion hotspot (Fig. 5, S2), our data are in good agreement with previously published data by Peters et al. (2021) and confirm a rather heterogeneous contribution of variable mantle domains displaying heterogeneous  $^{182}\text{W}$  ( $\mu^{182}\text{W} = -9.6 \pm 4.6$  to  $0.0 \pm 6.3$ ) at given  $^{143}\text{Nd}$ - $^{176}\text{Hf}$  isotope compositions, respectively. To explain the observed heterogeneity of  $^{182}\text{W}$ ,  $^{142}\text{Nd}$  and  $^3\text{He}/^4\text{He}$  isotope systematics, Peters et al. (2021) have proposed a complex model that involves mixing of a core equilibrated, enriched Hadean magma ocean remnant, depleted magma ocean relics and small amounts of recycled Hadean mafic crust. While our samples from PDF with clear  $^{182}\text{W}$  deficits might indeed indicate contributions of a W-rich, primordial component having interacted with the Earth's core, the concurrent DUPAL-flavor in Sr-Pb isotope space also suggests contributions of shallower crustal reservoirs (Bosch et al., 2008; Regelous et al., 2009). Investigating fresh volcanic glass samples from the Mid-Atlantic Ridge at 26°S and off-axis seamounts, Regelous et al. (2009) linked the DUPAL anomaly to shallow level incorporation of disrupted lower-continental crust and lithospheric mantle fragments. In the case of the La Réunion hotspot, these models are also supported by the presence of Archean zircons found in Mauritius lavas (Ashwal et al., 2017) and a recent study by Nauret et al. (2019), identifying the presence of ancient crustal fragments at shallower depths. We note that our suggestions are also in line with recent SCLM models claiming the presence of disrupted and metasomatized SCLM domains beneath several intraplate volcanoes, a viable alternative source for geochemical signatures that were previously ascribed to lower mantle reservoirs (e.g., Belay et al., 2019; Guimarães et al., 2020). By analogy to the nearby Kaapvaal Craton (e.g., Puchtel et al., 2016; Tusch et al., 2021a), the presence of  $^{182}\text{W}$  deficits in La Réunion basalts may thus also call for the recycling of lower-crustal Hadean to early Archean restites from prolonged TTG formation that significantly contributed to magmatism in the Indian ocean. Following the model of Tusch et al. (2021a), mixing of such material with classical mantle end-members can readily account for the observed heterogeneous  $^{182}\text{W}$ ,  $^{142}\text{Nd}$  and long-lived radiogenic isotope systematics in OIBs like those from La Réunion. However, as moderately high and exceptionally uniform  $^3\text{He}/^4\text{He}$  ratios of  $\sim 13 R_A$  (Füri et al., 2011) are apparently inconsistent with a contribution of crustal material it has been previously suggested that the source has been recently enriched by unradiogenic helium through diffusion (e.g., Regelous et al., 2009 and references therein).

In contrast to La Réunion, the picrites from the proto-Iceland plume (PIP) display a large range of trace element and radiogenic isotope compositions (Stuart et al., 2003; Starkey et al., 2009; Willhite et al., 2019). Although lavas from the PIP display overall depleted long-lived radiogenic isotope compositions similar to MORB, recent studies have imaged a plume structure underneath Iceland that tilts to the NNW at 350–400 km depth, reaching beneath eastern Greenland (Celli et al., 2021). Most importantly, samples from the PIP display the highest  $^3\text{He}/^4\text{He}$  ratios measured so far (as high as 50  $R_A$ ) (Stuart et al., 2003; Starkey et al., 2009; Willhite et al., 2019). This likely reflects the pollution of plume-entrained mantle by volatiles from He-rich high  $^3\text{He}/^4\text{He}$  deep mantle domains (e.g., Starkey et al., 2009; Dale et al., 2009). Alternatively, the PIP samples a unique, deep mantle reservoir that has remained isolated throughout most of Earth's history (Willhite et al., 2019). Previous



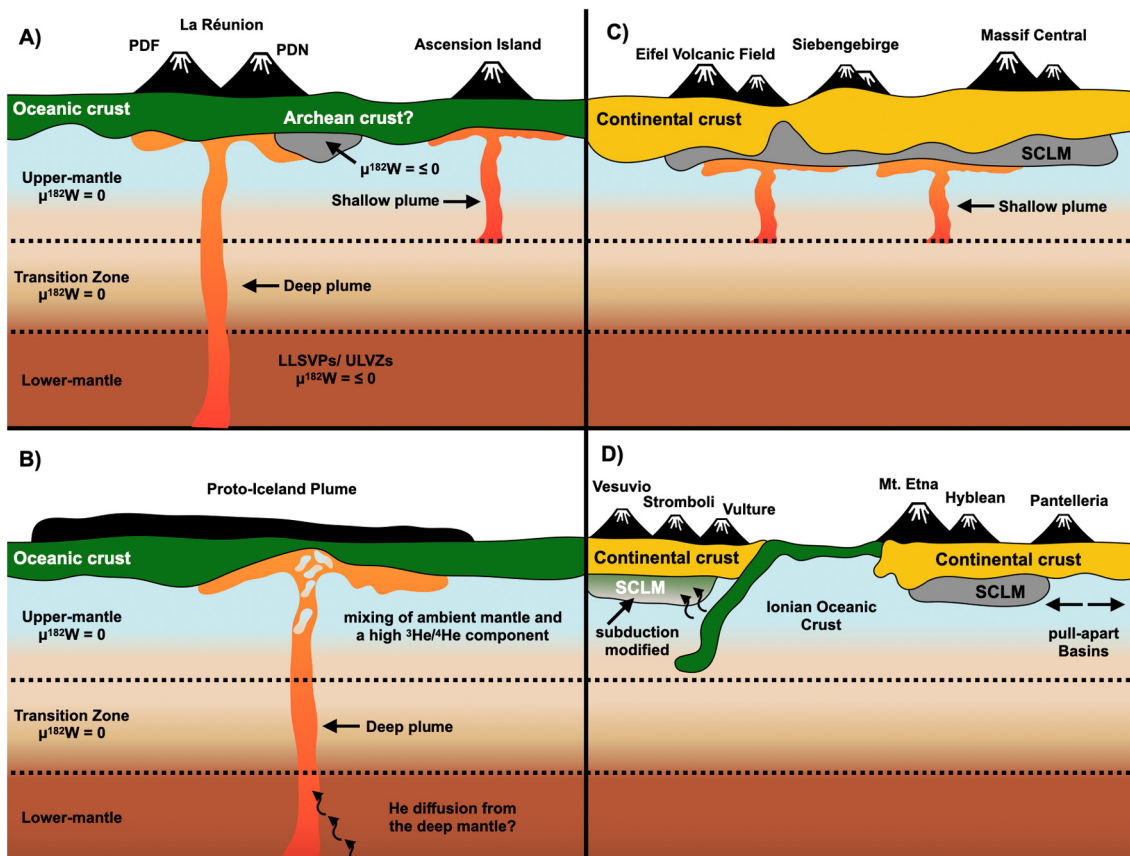


**Fig. 7.** Schematic sketch illustrating the geodynamic implications gained by  $^{182}\text{W}$  isotope data from this study and the literature. A) Deep plumes as a carrier of negative  $^{182}\text{W}$  anomalies; a heterogeneous distribution of LLSVP and ULVZ material within the plume is responsible for the heterogeneous  $^{182}\text{W}$  compositions of both volcanic edifices (e.g., Mundl-Petermeier et al., 2019, 2020); Alternatively, recycled Archean crustal materials that account for the Pb-DUPAL flavor of PDF volcanic samples (Bosch et al., 2008) also carry anomalous  $^{182}\text{W}$  signatures. The compositions of shallow-plume related Ascension Island lavas are controlled by the upper-mantle or potentially reflect primordial signatures, present as relicts from the interacting St. Helena and Tristan plumes (e.g., Zhang et al., 2020). B) Data for samples from Baffin Bay and Padloping Island indicate a dominant influence of upper mantle material (e.g., Stuart et al., 2003; Starkey et al., 2009); the absence of deficient  $^{182}\text{W}$  compositions despite high  $^3\text{He}/^4\text{He}$  ratios (Starkey et al., 2009) further indicates that the W and He budgets are apparently decoupled (Mundl-Petermeier et al., 2019, 2020; Jackson et al., 2020). C) For the CEVP, our data are in good agreement with noble-gas compositions (e.g., Bekaert et al., 2019) and detailed evaluations of long-lived radiogenic isotope compositions that suggest a common mantle reservoir (CMR), located within the upper mantle underneath the CEVP. D) Similar to the CEVP, seismic studies have provided evidence for a shallow-plume origin of Etna volcanism (e.g., Montelli et al., 2006) and radiogenic isotope compositions are similar to the CMR (Lustrino and Wilson, 2007). The largely homogeneous  $^{182}\text{W}$  composition of all settings analyzed here, overlapping with the modern upper-mantle value, does not indicate contributions of primordial material from the lower-mantle.

$^{182}\text{W}$  analyses of PIP basalts have yielded contrasting results (e.g., Rizo et al., 2016; Mundl-Petermeier et al., 2019, 2020). A study by Rizo et al. (2016) has reported exceptionally high  $^{182}\text{W}$  excesses in samples from Padloping Island (up to  $\mu^{182}\text{W} = +48.4 \pm 4.6$  ppm) and attributed this to the preservation of a depleted reservoir that formed through Hadean silicate differentiation. The same study reported  $^{182}\text{W}$  excesses of similar magnitude in modern volcanic rocks from the Ontong-Java Plateau (OJP) that, however, were inconsistent with previous measurements by Willbold et al. (2011) and more recent measurements of stratigraphically similar rocks from the OJP (Kruijer and Kleine, 2018). This follow-up study postulated that the excesses reported by Rizo et al. (2016) might be analytical artifacts induced by nuclear field shift effects (Kruijer and Kleine, 2018). Alternatively, Mundl-Petermeier et al. (2020) suggested that the elevated  $^{182}\text{W}$  isotope compositions could be inherited from the Archean basement by metasomatic fluids. To clarify this controversy, we have analyzed four high  $^3\text{He}/^4\text{He}$  PIP picrites from Durban Island and Padloping Island. The  $\mu^{182}\text{W}$  values for our PIP samples with undisturbed elemental W budgets (canonical W/Th) display a narrow range from  $-4.5 \pm 8.7$  to  $+2.2 \pm 6.3$  ppm (Table 2, Fig. 6), clearly demonstrating that the W isotope compositions of the parental sources are indistinguishable from the inferred composition of modern upper mantle. Metasomatic agents that carry  $^{182}\text{W}$  excesses appear not to account for

the extreme anomalies found by Rizo et al. (2016), because sample DUR 1 with elevated W/Th also shows modern upper mantle-like  $\mu^{182}\text{W}$  (Fig. 5). The absence of a W isotope anomaly in the highest  $^3\text{He}/^4\text{He}$  basalts available provide no clear support for previous claims for a unique high  $^3\text{He}/^4\text{He}$  reservoir in the deep mantle that has remained isolated from convective mixing since the first few 10s Myr (e.g., Graham, 2002; Jackson et al., 2020). Instead, the data are more consistent with models where He isotopes are decoupled from other isotope systems either by mixing of He-rich deep mantle with depleted and enriched mantle components entrained by the plume, or by long-term diffusion of He from a primordial volatile-rich reservoir (Starkey et al., 2009).

#### 5.4. Origin of W isotope compositions in intraplate lavas derived from shallow mantle plumes

In contrast to classical plume settings discussed above, the origin of Ascension Island volcanism is still highly debated. While geochemical studies have indicated highly heterogeneous mantle sources (e.g., Paulick et al., 2010; Zhang et al., 2020), seismic studies have yielded contrasting results in that both deep- as well as shallow-plume origins have been suggested (French and Romanowicz, 2015 and references therein). Basalts from Ascension Island and the surrounding MAR segments (e.g., Paulick et al.,

2010) can be explained by binary mixing between depleted mantle and HIMU reservoirs (Zhang et al., 2020 and references therein). The  $^{143}\text{Nd}/^{144}\text{Nd}$  and  $^{176}\text{Hf}/^{177}\text{Hf}$  compositions of the samples analyzed here represent the enriched endmember that contributed to nearly all eruptive stages of Ascension volcanism (Paulick et al., 2010) (Fig. 3). Irrespective of fluid alteration (which affected sample ASD 16), the  $^{182}\text{W}$  composition of our samples is homogenous with values ranging from  $\mu^{182}\text{W} = -0.2 \pm 3.5$  to  $+0.1 \pm 4.7$  ppm (Table 2, Fig. 6). We can not fully exclude that magmatism on Ascension Island, that is located on the edge of the African LLSVP (Fig. 1), may tap a deep plume-related magma source or interacts with non-anomalous  $^{182}\text{W}$  plumes such as the nearby plumes of St. Helena and Tristan (Zhang et al., 2020; Mundl-Petermeier et al., 2020; Jackson et al., 2020). However, the combination of our data with published  $^3\text{He}/^4\text{He}$  data (6.3 to 7.3  $R_A$ ; Ammon et al., 2009) indicates a major control of upper mantle reservoirs on the compositions of Ascension Island lavas (Paulick et al., 2010; Fig. 7). This is also in good agreement with recent seismic data indicating a shallow-plume origin (French and Romanowicz, 2015).

Seismic studies of the CEVP have revealed shallow plume structures rooted at the mantle transition zone (Ritter et al., 2001). However, the presence of deep rooted plume structures still remains debated (e.g., Granet et al., 1995; French and Romanowicz, 2015). Based on a similar long-lived radiogenic isotope compositions of lavas sampled across all eruptive centers of the CEVP, several studies have suggested a common mantle reservoir that is accessible for partial melting beneath Europe (Common Mantle or European Asthenospheric Reservoir (CMR or EAR); e.g., Hoernle et al., 1995; Lustrino and Wilson, 2007). Considering the Sr-Hf-Nd-Pb isotope compositions of CEVP lavas, the CMR comprises a range of very different mantle endmembers, covering EM I, EM II and HIMU-like compositions (Lustrino and Wilson, 2007). While EM I- and EM II-like endmembers may reflect contributions from younger crustal material that has been mixed into the mantle during orogenic events (e.g. the Variscan orogeny), the HIMU-like endmember may have interacted with CMR-like asthenospheric melts that tapped metasomatized SCLM (Jung et al., 2011; Lustrino and Wilson, 2007; Pfänder et al., 2018). However, the origin of the HIMU-like component in CEVP lavas is still debated and an asthenospheric as well as an SCLM origin have been suggested (e.g., Lustrino and Wilson, 2007). Rather low  $^3\text{He}/^4\text{He}$  ( $\sim 6 R_A$ ) ratios measured in mantle xenoliths and gas from Eifel springs (Dunai and Baur, 1995; Bekaert et al., 2019 and references therein) further suggest an upper- rather than a lower mantle origin.

The continental intraplate volcanic rocks of the CEVP analyzed here display no resolvable  $^{182}\text{W}$  deficits (Eifel Volcanic Field:  $\mu^{182}\text{W} = -0.8 \pm 2.6$  ppm to  $\mu^{182}\text{W} = +3.9 \pm 4.0$  ppm; Massif Central:  $\mu^{182}\text{W} = -4.4 \pm 3.6$  ppm to  $\mu^{182}\text{W} = 0.0 \pm 3.7$  ppm; Siebengebirge:  $\mu^{182}\text{W} = +0.1 \pm 4.1$  ppm to  $\mu^{182}\text{W} = +1.1 \pm 4.1$  ppm). Therefore, our  $^{182}\text{W}$  isotope perspective provides no evidence for the contribution of long-term isolated mantle material (Table 2, Fig. 6). Notably, assimilation of continental crust during slow magma ascent may modify the original geochemical composition of continental intraplate melts. However, the presence of mantle nodules in volcanic rocks of the CEPV, their high MgO contents and their radiogenic isotope compositions argue for rapid magma ascent and little interaction with continental crust (e.g., Wörner et al., 1986; Schmicke et al., 2007; Lustrino and Wilson, 2007 and references therein). Considering radiogenic isotope compositions of the samples analyzed here (Table A-5, Fig. 3) and the review of CEVP volcanism by Lustrino and Wilson (2007), our data are in good agreement with models that propose contributions from shallow-plumes (Ritter et al., 2001 and references therein) and a dominant lithospheric control on the incompatible element budget of magmatic rocks from the CEVP, including that of W (Lustrino and Wilson, 2007; Pfänder et al., 2018) (Fig. 7C).

Collectively, the volcanic settings discussed above demonstrate that combined geochemical and seismic constraints can not always provide unambiguous evidence for a deep plume structure. Ascension Island and the CEVP are exemplary sites, where different seismic models permit different depths of mantle domains involved in magma generation (e.g., Montelli et al., 2006; French and Romanowicz, 2015; Granet et al., 1995; Ritter et al., 2001), despite resembling long-lived radiogenic isotope compositions similar to classical plume settings (e.g., Lustrino and Wilson, 2007; Paulick et al., 2010). This calls for the careful combination of multiple proxies such as W isotopes, seismic studies, long-lived radiogenic isotope- and noble gas compositions. We argue that this multi-proxy approach, now complemented by our new  $^{182}\text{W}$  data, provides strong evidence for a shallow plume origin of Ascension Island and CEVP volcanism that is broadly similar to the previously published models of Belay et al. (2019) and Guimarães et al. (2020).

##### 5.5. Tungsten isotope compositions in intraplate lavas from the Italian Magmatic Province associated with subduction

Compositionally, volcanic rocks from the Tyrrhenian Sea region nearly cover the complete spectrum of mantle endmembers known to date (e.g., Lustrino and Wilson, 2007; Peccerillo, 2017). Throughout this study, we have investigated a variety of settings that include intraplate volcanic rocks (Mt Etna, Hyblean Plateau, Pantelleria) with Hf-Nd isotope compositions similar to the CMR (Fig. 3) as well as samples indicative of subduction-related crustal contributions (Stromboli, Vesuvio, Vulture) (Table A-5, Fig. 3). Previous studies have suggested the influence of a mantle plume (Hoernle et al., 1995) as well as inflow of African asthenospheric material (Trua et al., 2003). However, with  $^{182}\text{W}$  compositions in a range from  $\mu^{182}\text{W} = -4.5 \pm 2.9$  ppm to  $+2.8 \pm 4.3$  ppm (Table 2, Fig. 6), we do not find evidence for a significant contribution of anomalous lower mantle material to the magma source of Mt. Etna and Pantelleria. Considering the subduction-controlled settings of Mt. Vesuvio and Stromboli, and to a lesser extent of Mt. Vulture, our samples generally reveal similar results with  $^{182}\text{W}$  compositions in a range from  $\mu^{182}\text{W} = -2.2 \pm 3.4$  to  $-0.4 \pm 2.9$  ppm (Table 2, Fig. 6). Our results are further in line with the absence of elevated  $^3\text{He}/^4\text{He}$  ratios (2.2 to 6  $R_A$ , e.g., Martelli et al., 2008). However, slightly deficient  $^{182}\text{W}$  compositions in one sample from Vesuvio ( $\mu^{182}\text{W} = -4.5 \pm 2.9$  ppm) might indicate the influence of ancient material, but this needs further investigation. Our samples from Etna, Pantelleria and the Hyblean Plateau, that are the most likely candidates for contributions of deep plume material, also display modern upper mantle-like  $^{182}\text{W}$  compositions.

The magmas of the Hyblean Plateau (Trua et al., 1998) show evidence for a SCLM component enriched by carbonatite metasomatism. Such a contribution was recently discovered also at Mt. Etna on the basis of HFS elements (Bragagni et al., 2022). The lithospheric mantle below Sicily, which influences magmatism of the Hyblean plateau and Etna, shows model ages attesting melt depletion events that occurred in the Archean or earlier (Sapienza et al., 2007), while carbonatite metasomatism was likely much more recent (Trua et al., 1998). The lack of any anomalous  $^{182}\text{W}$  compositions at Etna and the Hyblean argues against an ancient origin of the ambient SCLM. Pantelleria shows no sign of SCLM contribution indicating a purely asthenospheric mantle source (Avanzinelli et al., 2014; Bragagni et al., 2022). The absence of anomalous  $^{182}\text{W}$  composition is consistent with an origin of the magmas from Pantelleria from the upper mantle due to passive upwelling resulting from lithospheric stretching with no evidence for the presence of a deep-seated mantle plume (see also Avanzinelli et al., 2014) as a whole, our data indicate that the local upper mantle and the SCLM beneath southern Italy do not carry anomalous  $^{182}\text{W}$ , similar to what observed in other volcanoes of the CMR. In absence of

a deep plume source at Vesuvio, we rather suggest, that CO<sub>2</sub>-rich fluids/melt released during subduction of ancient material lead to secondary redistribution of W in the source region of Mt. Vesuvio lavas.

## 6. Conclusions

This study presents the first comprehensive <sup>182</sup>W dataset for intraplate volcanic rocks involving shallow plume, continental intraplate and subduction-related settings as well as new data for deep-rooted mantle plumes. In Fig. 7 we illustrate the geodynamic implications and conclusions based on the data gained throughout this study. In summary, the following key findings that emerge from our study are:

- 1) Data for deep plume-related La Réunion lavas indicate <sup>182</sup>W heterogeneities that are in good agreement with previously reported data by Peters et al. (2021). While the heterogeneous distribution of lower-mantle material within the rising plume would certainly provide a viable explanation, the combination of our <sup>182</sup>W data and previously published <sup>3</sup>He/<sup>4</sup>He compositions only slightly overlap with previously proposed correlation trends (Mundl-Petermeier et al., 2020; Jackson et al., 2020). By analogy to a recent study on <sup>182</sup>W compositions in Archean rocks from the Kaapvaal Craton (Tusch et al., 2021a), we alternatively suggest that the <sup>182</sup>W-poor mantle tapped by the PDF volcanism may result from the incorporation of recycled restites from Hadean protocrust within the upper mantle. This model is in line with the strong DUPAL signature in the Pb isotope record of the PDF lavas (Fig. 7A) but conflicts with seismic studies that image a clear plume structure anchored in the lower mantle (French and Romanowicz, 2015).
- 2) The high temperature picritic basalts erupted by the early Iceland plume do not display resolvable <sup>182</sup>W anomalies. The absence of <sup>182</sup>W anomalies provide no clear support for suggestions of a long-isolated primordial reservoir present at the core-mantle boundary but are consistent with He pollution of entrained mantle (e.g., Starkey et al., 2009) (Fig. 7B), as <sup>182</sup>W and <sup>3</sup>He/<sup>4</sup>He are decoupled.
- 3) The absence of <sup>182</sup>W anomalies in shallow plume-sourced Ascension Island samples indicates an upper mantle control on the <sup>182</sup>W composition and no contributions from anomalous lower mantle reservoirs (Fig. 7A), even though Ascension Island is located on the margin of the African LLSVP (Fig. 1).
- 4) A largely homogenous <sup>182</sup>W composition of our samples from the CEVP is in good agreement with noble gas data suggesting an upper mantle origin (Fig. 7C), and a strong influence of lithospheric components. These data also suggest the absence of anomalous <sup>182</sup>W domains in the mantle beneath Central Europe.
- 5) The <sup>182</sup>W budget of intraplate volcanism within the IMP is largely controlled by shallow upper mantle components such as the CMR (Fig. 7D), with contributions from relatively recent SCLM at the Hyblean Plateau and Mt. Etna, and variable (carbonate-rich vs. carbonate-poor) subduction-related components in Vesuvio and Stromboli, and to a lesser extent in Mt. Vulture.
- 6) Our data support models claiming that anomalous <sup>182</sup>W compositions are confined to lower mantle reservoirs and do not occur in shallow mantle plumes. However, the combination of our <sup>182</sup>W data and previously published Sr-Nd-Hf-Pb-He isotope data might indicate recycled Hadean crustal fragments as a potential source of deficient W isotope compositions in La Réunion lavas.
- 7) The widespread absence of <sup>182</sup>W anomalies in basalts from the European portion of the northern hemisphere can also

be explained by the absence of isotopically anomalous and isolated domains in the deep mantle beneath the European hemisphere, as also suggested by geophysical evidence (e.g., French and Romanowicz, 2015).

- 8) In combination with previously published data on OIBs, our newly gained data on highly variable geodynamic settings provide strong evidence for a geochemically stratified mantle. Although further investigations are necessary, combined He-W systematics suggest the lower-mantle to be the host region of primordial reservoirs within the earth's modern mantle (e.g., Graham et al., 2002).

## CRediT authorship contribution statement

**Mike W. Jansen:** Conceptualization, Formal analysis, Investigation, Methodology, Validation, Visualization, Writing – original draft. **Jonas Tusch:** Formal analysis, Investigation, Methodology, Resources, Validation, Writing – review & editing. **Carsten Münker:** Conceptualization, Funding acquisition, Methodology, Resources, Supervision, Writing – review & editing. **Alessandro Bragagni:** Conceptualization, Resources, Writing – review & editing. **Riccardo Avanzinelli:** Conceptualization, Resources, Writing – review & editing. **Filippo Mastroianni:** Investigation, Resources. **Finlay M. Stuart:** Conceptualization, Resources, Writing – review & editing. **Florian Kurzweil:** Conceptualization, Writing – review & editing.

## Declaration of competing interest

The authors declare that they have no known competing financial interests or personal relationships that could have appeared to influence the work reported in this paper.

## Acknowledgements

Financial support for this study was provided by the European Research Council (ERC grant no. 669666) to C.M. Frank Wombacher is thanked for his help performing trace element analysis using the ThermoFisher iCap-Q at the University of Cologne. We thank Dieter Garbe-Schönberg, Ulrike Westernströer and the technical staff of the ICP-MS laboratory at CAU Kiel for quadrupole ICP-MS analysis. Eric Hasenstab and Mario Fischer-Gödde are thanked for the numerous fruitful discussions during the course of this study. We thank Sandro Conticelli and Lorella Francalanci for providing samples from Vesuvio, Vulture, Pantelleria and Stromboli. Comments by Valerie Finlayson, one anonymous reviewer and journal editor Rajdeep Dasgupta helped to improve the manuscript.

## Appendix A. Supplementary material

Supplementary material related to this article can be found online at <https://doi.org/10.1016/j.epsl.2022.117507>.

## References

- Ammon, K., Dunai, T.J., Stuart, F.M., Meriaux, A.-S., Gayer, E., 2009. Cosmogenic <sup>3</sup>He exposure ages and geochemistry of basalts from Ascension Island, Atlantic Ocean. *Quat. Geochronol.* 4, 423–430.
- Ashwal, L.D., Wiedenbeck, M., Torsvik, T.H., 2017. Archean zircons in Miocene oceanic hotspot rocks establish ancient continental crust beneath Mauritius. *Nat. Commun.* 14089.
- Avanzinelli, R., Braschi, E., Marchionni, S., Bindi, L., 2014. Mantle melting in within-plate continental settings: Sr-Nd-Pb and U-series isotope constraints in alkali basalts from the Sicily Channel (Pantelleria and Linosa Islands, Southern Italy). *Lithos* 188, 113–129.
- Avanzinelli, R., Casalini, M., Elliott, T., Conticelli, S., 2018. Carbon fluxes from subducted carbonates revealed by uranium excess at Mount Vesuvius, Italy. *Geology* 46 (3), 259–262. <https://doi.org/10.1130/G39766.1>.



- Bekaert, D.V., Broadley, M.W., Caracausi, A., Marty, B., 2019. Novel insights into the degassing history of Earth's mantle from high precision noble gas analysis of magmatic gas. *Earth Planet. Sci. Lett.* 525, 115766. <https://doi.org/10.1016/j.epsl.2019.115766>.
- Belay, I.G., Tanaka, R., Kitagawa, H., Kobayashi, K., Nakamura, E., 2019. Origin of ocean island basalts in the West African passive margin without mantle plume involvement. *Nat. Commun.* 10 (1), 1–12.
- Bosch, D., Blichert-Toft, J., Moynier, F., Nelson, B.K., Telouk, P., Gillot, P.Y., Albarède, F., 2008. Pb, Hf and Nd isotope compositions of the two Réunion volcanoes (Indian Ocean): a tale of two small-scale mantle "blobs"? *Earth Planet. Sci. Lett.* 265, 748–765. <https://doi.org/10.1016/j.epsl.2007.11.018>.
- Bouvier, A., Vervoort, J.D., Patchett, P.J., 2008. The Lu-Hf and Sm-Nd isotopic composition of CHUR: constraints from unequilibrated chondrites and implications for the bulk composition of terrestrial planets. *Earth Planet. Sci. Lett.* 237, 48–57.
- Bragagni, A., Avanzinelli, R., Freymuth, H., Francalanci, L., 2014. Recycling of crystal mush-derived melts and short magma residence times revealed by U-series disequilibria at Stromboli volcano. *Earth Planet. Sci. Lett.* 404, 206–219.
- Bragagni, A., Mastroianni, F., Münker, C., Conticelli, S., Avanzinelli, R., 2022. A carbon-rich lithospheric mantle as a source for the large CO<sub>2</sub> emissions of Etna volcano (Italy). *Geology*.
- Carlson, R.W., Boyet, M., 2008. Composition of the Earth's interior: the importance of early events. *Philos. Trans. R. Soc. A, Math. Phys. Eng. Sci.* 366, 4077–4103. <https://doi.org/10.1098/rsta.2008.0166>.
- Celli, N.L., Lebedev, S., Schaeffer, A.J., Gaina, C., 2021. The tilted Iceland Plume and its effect on the North Atlantic evolution and magmatism. *Earth Planet. Sci. Lett.* 569, 117048.
- Dale, C.W., Pearson, D.G., Starkey, N.A., Stuart, F.M., Ellam, R.M., Larsen, L.M., Fitton, J.G., Macpherson, C.G., 2009. Osmium isotopes in Baffin Island and West Greenland picrites: Implications for the 187Os/188Os composition of the convecting mantle and the nature of high 3He/4He mantle. *Earth Planet. Sci. Lett.* 278 (3–4), 267–277.
- Dunai, T.J., Baur, H., 1995. Helium, neon, and argon systematics of the European subcontinental mantle: implications for its geochemical evolution. *Geochim. Cosmochim. Acta* 59 (13), 2767–2783.
- Dupré, B., Allègre, C.J., 1983. Pb–Sr isotope variation in Indian Ocean basalts and mixing phenomena. *Nature* 303, 142–146.
- French, S.W., Romanowicz, B., 2015. Broad plumes rooted at the base of the Earth's mantle beneath major hotspots. *Nature* 525, 95.
- Füri, E., Hilton, D.R., Murton, B.J., Hémond, C., Dymont, J., Day, J.M.D., 2011. Helium isotope variations between Réunion Island and the Central Indian Ridge (17°–21°S): new evidence for ridge–hot spot interaction. *J. Geophys. Res.* 116. <https://doi.org/10.1029/2010JB007609>.
- Graham, D.W., 2002. Noble gas isotope geochemistry of mid-ocean ridge and ocean island basalts: characterization of mantle source reservoirs. *Rev. Mineral. Geochem.* 47 (1), 247–317. <https://doi.org/10.2138/rmg.2002.47.8>.
- Granet, M., Wilson, M., Achauer, U., 1995. Imaging a mantle plume beneath the French Massif Central. *Earth Planet. Sci. Lett.* 136, 281–296.
- Guimarães, A.R., Fitton, J.G., Kirstein, L.A., Barfod, D.N., 2020. Contemporaneous intraplate magmatism on conjugate South Atlantic margins: a hotspot conundrum. *Earth Planet. Sci. Lett.* 536, 116147.
- Hart, S.R., Hauri, E.H., Oschmann, L.A., Whitehead, J.A., 1992. Mantle plumes and entrainment: isotopic evidence. *Science* 256 (5056), 517–520.
- Hoernle, K.A.J., Zhang, Y.-S., Graham, D., 1995. Seismic and geochemical evidence for large-scale mantle upwelling beneath the eastern Atlantic and western and central Europe. *Nature* 374, 34.
- Hofmann, A.W., 2003. Sampling mantle heterogeneity through oceanic basalts: isotopes and trace elements. *Treatise Geochem.* 2, 568.
- Jackson, M.G., Blichert-Toft, J., Halldórsson, S.A., Mundl-Petermeier, A., Bizimis, M., Kurz, M.D., Price, A.A., Harðardóttir, S., Willhite, L.N., Breddam, K., 2020. Ancient helium and tungsten isotopic signatures preserved in mantle domains least modified by crustal recycling. *Proc. Natl. Acad. Sci.* 117, 30993–31001.
- Jung, S., Pfänder, J.A., Brauns, M., Maas, R., 2011. Crustal contamination and mantle source characteristics in continental intra-plate volcanic rocks: Pb, Hf and Os isotopes from central European volcanic province basalts. *Geochim. Cosmochim. Acta* 75, 2664–2683.
- König, S., Münker, C., Schuth, S., Garbe-Schönberg, D., 2008. Mobility of tungsten in subduction zones. *Earth Planet. Sci. Lett.* 274, 82–92.
- König, S., Münker, C., Hohl, S., Paulick, H., Barth, A.R., Lagos, M., Pfänder, J., Büchl, A., 2011. The Earth's tungsten budget during mantle melting and crust formation. *Geochim. Cosmochim. Acta* 75, 2119–2136.
- Kröner, A., Hoffmann, J.E., Hangqiang, X., Münker, C., Hegner, E., Yusheng, W., Hofmann, A., Liu, D., Jinhui, Y., 2014. Generation of early Archean grey gneisses through melting of older crust in the eastern Kaapvaal craton, southern Africa. *Precambrian Res.* 255, 823–846.
- Kruijer, T.S., Kleine, T., 2018. No 182W excess in the Ontong Java Plateau source. *Chem. Geol.* 485, 24–31.
- Kurzweil, F., Münker, C., Tusch, J., Schoenberg, R., 2018. Accurate stable tungsten isotope measurements of natural samples using a 180W–183W double-spike. *Chem. Geol.* 476, 407–417.
- Kurzweil, F., Münker, C., Grupp, M., Braukmüller, N., Fechtner, L., Christian, M., Hohl, S.V., Schoenberg, R., 2019. The stable tungsten isotope composition of modern igneous reservoirs. *Geochim. Cosmochim. Acta* 251, 176–191.
- Kurzweil, F., Münker, C., Hoffmann, J.E., Tusch, J., Schoenberg, R., 2020. Stable W isotope evidence for redistribution of homogeneous W-182 anomalies in SW Greenland. *Geochem. Perspect. Lett.* 14, 53–58.
- Liu, J., Pearson, D.G., Chacko, T., Luo, Y., 2018. A reconnaissance view of tungsten reservoirs in some crustal and mantle rocks: implications for interpreting W isotopic compositions and crust–mantle W cycling. *Geochim. Cosmochim. Acta* 223, 300–318.
- Lustrino, M., Wilson, M., 2007. The circum-Mediterranean anorogenic Cenozoic igneous province. *Earth-Sci. Rev.* 81, 1–65.
- Martelli, M., Nuccio, P.M., Stuart, F.M., Di Liberto, V., Ellam, R.M., 2008. Constraints on mantle source and interactions from He–Sr isotope variation in Italian Plio-Quaternary volcanism. *Geochim. Geophys. Geosyst.*, Q02001. <https://doi.org/10.1029/2007GC001730>.
- Montelli, R., Nolet, G., Dahlen, F.A., Masters, G., 2006. A catalogue of deep mantle plumes: new results from finite-frequency tomography. *Geochim. Geophys. Geosyst.* 7 (11).
- Mukhopadhyay, S., 2012. Early differentiation and volatile accretion recorded in deep-mantle neon and xenon. *Nature* 486, 101–104. <https://doi.org/10.1038/nature11141>.
- Mundl, A., Touboul, M., Jackson, M.G., Day, J.M.D., Kurz, M.D., Lekic, V., Helz, R.T., Walker, R.J., 2017. Tungsten-182 heterogeneity in modern ocean island basalts. *Science* 356 (6366), 66–69. <https://doi.org/10.1126/science.1241799>.
- Mundl-Petermeier, Walker, R.J., Fischer, R.A., Lekic, V., Jackson, M.G., Kurz, M.D., 2020. Anomalous 182W in high 3He/4He ocean island basalts: fingerprints of Earth's core? *Geochim. Cosmochim. Acta* 271, 194–211.
- Mundl-Petermeier, A., Walker, R.J., Jackson, M.G., Blichert-Toft, J., Kurz, M.D., Halldórsson, S.A., 2019. Temporal evolution of primordial tungsten-182 and 3He/4He signatures in the Iceland mantle plume. *Chem. Geol.* 525, 245–259. <https://doi.org/10.1016/j.chemgeo.2019.07.026>.
- Nakanishi, N., Giuliani, A., Carlson, R.W., Horan, M.F., Woodhead, J., Pearson, D.G., Walker, R.J., 2021. Tungsten-182 evidence for an ancient kimberlite source. *Proc. Natl. Acad. Sci.* 118 (23).
- Naurel, F., Famin, V., Vlastélic, I., Gannoun, A., 2019. A trace of recycled continental crust in the Réunion hotspot. *Chem. Geol.* 524, 67–76.
- Newsom, H.E., Sims, K.W., Noll Jr, P.D., Jaeger, W.L., Maehr, S.A., Beserra, T.B., 1996. The depletion of tungsten in the bulk silicate Earth: constraints on core formation. *Geochim. Cosmochim. Acta* 60 (7), 1155–1169.
- Nielson, D.L., Sibbett, B.S., 1996. Geology of Ascension Island, South Atlantic Ocean. *Geothermics* 25, 427–448.
- Noll Jr, P.D., Newsom, H.E., Leeman, W.P., Ryan, J.G., 1996. The role of hydrothermal fluids in the production of subduction zone magmas: evidence from siderophile and chalcophile trace elements and boron. *Geochim. Cosmochim. Acta* 60 (4), 587–611.
- Paulick, H., Münker, C., Schuth, S., 2010. The influence of small-scale mantle heterogeneities on Mid-Ocean Ridge volcanism: evidence from the southern Mid-Atlantic Ridge (7°30'S to 11°30'S) and Ascension Island. *Earth Planet. Sci. Lett.* 296, 299–310. <https://doi.org/10.1016/j.epsl.2010.05.009>.
- Pecceirillo, A., 2017. *Cenozoic Volcanism in the Tyrrhenian Sea Region*. Springer.
- Peters, B.J., Carlson, R.W., Day, J.M.D., Horan, M.F., 2018. Hadean silicate differentiation preserved by anomalous 142Nd/144Nd ratios in the Réunion hotspot source. *Nature* 555, 89–93. <https://doi.org/10.1038/nature25754>.
- Peters, B.J., Mundl-Petermeier, A., Carlson, R.W., Walker, R.J., Day, J., 2021. Combined lithophile-siderophile isotopic constraints on Hadean processes preserved in ocean island basalt sources. *Geochim. Geophys. Geosyst.*, e2020GC009479.
- Pfänder, J.A., Jung, S., Klügel, A., Münker, C., Romer, R.L., Sperner, B., Rohrmüller, J., 2018. Recurrent local melting of metasomatised lithospheric mantle in response to continental rifting: constraints from basanites and nephelinites/melilitites from SE Germany. *J. Petrol.* 59, 667–694. <https://doi.org/10.1093/petrology/egy041>.
- Puchtel, I.S., Blichert-Toft, J., Touboul, M., Horan, M.F., Walker, R.J., 2016. The coupled 182W–142Nd record of early terrestrial mantle differentiation. *Geochim. Geophys. Geosyst.* 17, 2168–2193.
- Regelous, M., Niu, Y., Abouchami, W., Castillo, P.R., 2009. Shallow origin for South Atlantic Dupal Anomaly from lower continental crust: geochemical evidence from the Mid-Atlantic Ridge at 26 S. *Lithos* 112, 57–72.
- Reifenröther, R., Münker, C., Scheibner, B., 2021. Evidence for tungsten mobility during oceanic crust alteration. *Chem. Geol.* 584, 120504.
- Reifenröther, R., Münker, C., Paulick, H., Scheibner, B., 2022. Alteration of abyssal peridotites is a major sink in the W geochemical cycle. *Geochim. Cosmochim. Acta*.
- Ritter, J.R.R., Jordan, M., Christensen, U.R., Achauer, U., 2001. A mantle plume below the Eifel volcanic fields, Germany. *Earth Planet. Sci. Lett.* 186, 7–14.
- Rizo, H., Walker, R.J., Carlson, R.W., Horan, M.F., Mukhopadhyay, S., Manthos, V., Francis, D., Jackson, M.G., 2016. Preservation of Earth-forming events in the tungsten isotopic composition of modern flood basalts. *Science* 352, 809–812.
- Rizo, H., Andrault, D., Bennett, N.R., Humayun, M., Brandon, A., Vlastélic, I., Moine, B., Poirier, A., Bouhifd, M.A., Murphy, D.T., 2019. 182W evidence for core–mantle interaction in the source of mantle plumes. *Geochem. Perspect. Lett.* 11, 6–11.



- Sapienza, G.T., Griffin, W.L., O'Reilly, S.Y., Morten, L., 2007. Crustal zircons and mantle sulfides: Archean to Triassic events in the lithosphere beneath south-eastern Sicily. *Lithos* 96, 503–523.
- Schmincke, H.U., 2007. The Quaternary volcanic fields of the east and west Eifel (Germany). In: *Mantle Plumes*. Springer, Berlin, Heidelberg, pp. 241–322.
- Starkey, N.A., Stuart, F.M., Ellam, R.M., Fitton, J.G., Basu, S., Larsen, L.M., 2009. Helium isotopes in early Iceland plume picrites: constraints on the composition of high  $3\text{He}/4\text{He}$  mantle. *Earth Planet. Sci. Lett.* 277, 91–100. <https://doi.org/10.1016/j.epsl.2008.10.007>.
- Stuart, F.M., Lass-Evans, S., Fitton, J.G., Ellam, R.M., 2003. High  $3\text{He}/4\text{He}$  ratios in picritic basalts from Baffin Island and the role of a mixed reservoir in mantle plumes. *Nature* 424, 57–59. <https://doi.org/10.1038/nature01711>.
- Tappe, S., Budde, G., Stracke, A., Wilson, A., Kleine, T., 2020. The tungsten-182 record of kimberlites above the African superplume: exploring links to the core-mantle boundary. *Earth Planet. Sci. Lett.* 547, 116473.
- Tommasini, S., Heumann, A., Avanzinelli, R., Francalanci, L., 2007. The fate of high-angle dipping slabs in the subduction factory: an integrated trace element and radiogenic isotope (U, Th, Sr, Nd, Pb) study of Stromboli volcano, Aeolian Arc, Italy. *J. Petrol.* 48, 2407–2430.
- Touboul, M., Puchtel, I.S., Walker, R.J., 2012.  $182\text{W}$  evidence for long-term preservation of early mantle differentiation products. *Science* 80 (335), 1065–1069.
- Trua, T., Esperança, S., Mazzuoli, R., 1998. The evolution of the lithospheric mantle along the N. African Plate: geochemical and isotopic evidence from the tholeiitic and alkaline volcanic rocks of the Hyblean plateau, Italy. *Contrib. Mineral. Petrol.* 131 (4), 307–322.
- Trua, T., Serri, G., Marani, M.P., 2003. Lateral flow of African mantle below the nearby Tyrrhenian plate: geochemical evidence. *Terra Nova* 15, 433–440.
- Tusch, J., Sprung, P., van de Löcht, J., Hoffmann, J.E., Boyd, A.J., Rosing, M.T., Münker, C., 2019. Uniform  $182\text{W}$  isotope compositions in Eoarchean rocks from the Isua region, SW Greenland: the role of early silicate differentiation and missing late veneer. *Geochim. Cosmochim. Acta* 257, 284–310. <https://doi.org/10.1016/j.gca.2019.05.012>.
- Tusch, J., Hoffmann, E., Hasenstab, E., Münker, C., 2021a. Long-term preservation of Hadean protocrust in Earth's mantle. *Earth Space Sci. Open Arch.* <https://doi.org/10.1002/essoar.10507464.1>.
- Tusch, J., Münker, C., Hasenstab, E., Jansen, M., Marien, C.S., Kurzweil, F., Van Kraendonck, M.J., Smithies, H., Maier, W., Garbe-Schönberg, D., 2021b. Convective isolation of Hadean mantle reservoirs through Archean time. *Proc. Natl. Acad. Sci.* 118 (2).
- Vockenhuber, C., Oberli, F., Bichler, M., Ahmad, I., Quitté, G., Meier, M., Halliday, A.N., Lee, D.-C., Kutschera, W., Steier, P., Gehrke, R.J., Helmer, R.G., 2004. New half-life measurement of  $182\text{Hf}$ : improved chronometer for the early solar system. *Phys. Rev. Lett.* 93. <https://doi.org/10.1103/PhysRevLett.93.172501>.
- Willbold, M., Elliot, T., Moorbath, S., 2011. The tungsten isotopic composition of the Earth's mantle before the terminal bombardment. *Nature* 477, 195–198.
- Willhite, L.N., Jackson, M.G., Blichert-Toft, J., Bindeman, I., Kurz, M.D., Halldórsson, S.A., Harðardóttir, S., Gazel, E., Price, A.A., Byerly, B., Byerly, B.L., 2019. Hot and heterogeneous high- $3\text{He}/4\text{He}$  components: new constraints from proto-Iceland plume lavas from Baffin Island. *Geochem. Geophys. Geosyst.* 20 (12), 5939–5967.
- Wörner, G., Zindler, A., Staudigel, H., Schmincke, H.U., 1986. Sr, Nd, and Pb isotope geochemistry of Tertiary and Quaternary alkaline volcanics from West Germany. *Earth Planet. Sci. Lett.* 79 (1–2), 107–119.
- Zhang, H., Shi, X., Li, C., Yan, Q., Yang, Y., Zhu, Z., Zhang, H., Wang, S., Guan, Y., Zhao, R., 2020. Petrology and geochemistry of South Mid-Atlantic Ridge ( $19^{\circ}\text{S}$ ) lava flows: implications for magmatic processes and possible plume-ridge interactions. *Geosci. Front.* 11 (6), 1953–1973.